REGULATION OF THE WNT PATHWAY BY TGFβ AND DYRK2: MECHANISMS OF DISEASE AND SIGNAL TRANSDUCTION

By

Rubin Sam Baskir

Dissertation

Submitted to the Faculty of the

Graduate School of Vanderbilt University

in partial fulfillment of the requirements

for the degree of

DOCTOR OF PHILOSOPHY

in

Interdisciplinary Studies: Focus on Clinical and Cellular Biology

August, 2016

Nashville, Tennessee

Approved:

Ethan Lee, M.D., Ph.D.

Matthew John Tyska, Ph.D.

Stephen R. Hann, Ph.D.

John S. Penn, Ph.D.

For my parents

“So I saw that there is nothing better for a man than to enjoy his work, because that is his lot. For who can bring him to see what will happen after him?”

Ecclesiastes 3:22

ACKNOWLEDGEMENTS

Firstly, I'd like to thank my parents, Bruce and Janice, both of whom are doctors and both of whom received many more calls, and at times, many less calls, than I'm sure they expected. No matter what experiment didn't work or what project failed, they were tireless in their support and showed an unshakable faith in me that was invaluable. Education is paramount in our family, and I am only just beginning to understand and appreciate the sacrifices they made for their children to be able to pursue their dreams. Thanks also go to my elder brother Eli and younger sister Liza who taught me not to take this work too seriously - I am proud to see them grow into wonderful people. Next, I'd like to thank my friends in graduate school, Lehanna and Andrew, who I'm sure are as surprised as I am that I made it this far. They opened their home to me and were perfect hosts throughout the nearly 7 years I've known them. Thanks also go to my friends Amy and Joe, who were excellent council and have shown me what true friendship is. A special thanks goes out to the entire Lee lab, who had to put up with me. From those, Kenyi deserves special recognition, as I'm sure I bugged him the most and he carried it with grace. I'd also like to thank the members of my committee, who I know advocated for me and allowed this thesis to be made - gentlemen and scholars, all. Thanks too go to Roger Chalkley, Chris Wright, and Richard Hoover, who I know first-hand truly care for the students of Vanderbilt and are their strongest advocates. For Ethan, no amount of thanks is possible. He has been a gracious, kind, thoughtful, and above all, patient mentor. Science needs more people like him. The final thanks goes to my girlfriend, Hannah Hankins. Every day, I love and admire her more and every day, she is more lovely and admirable.

TABLE OF CONTENTS

LIST OF TABLES

LIST OF FIGURES

LIST OF ABBREVIATIONS

APC, adenomatous polyposis coli

ARM, Armadillo

ATP, adenosine triphosphate

BM-MSC, bone marrow-derived mesenchymal cells

CK1α, casein kinase 1

CoIP, co-immunoprecipitation

COPD, chronic obstructive pulmonary disease

CRC, colorectal cancer

CTNNB1, Catenin (Cadherin-Associated Protein), 1

dpp, decapentaplegic

DYRK, dual specificity tyrosine-regulated kinase

EC, endothelial cell

ECM, extracellular matrix

EDTA, ethylenediaminetetraacetic acid

ENU, *N*-ethyl-*N-nitrosourea*

ER, endoplasmic reticulum

FACS, fluorescence-activated cell sorting

FAP, familial adenomatous polyposis

FMO, fluorescent minus one

Fzd, Frizzled

GFP, green fluorescent protein

GSK3, glycogen synthase kinase-3

HEPES, 4-(2-hydroxyethyl)-1-piperazineethanesulfonic acid

HIPK, homeodomain-interacting protein kinase

HMG, High-mobility group

ICD, intracellular domain

ILD, interstitial lung disease

INDY, inhibitor of DYRK

IPF, idiopathic pulmonary fibrosis

KO, knock out

lacZ, β-galactosidase

LTR, long terminal repeat

Mad, Mothers against decapentaplegic

MADD, Mothers Against Drunk Driving

MAP, Mitogen-activated protein

MBS, Modified Barth's Saline

MBT, midblastula transition

MCR, mutation cluster region

Min, multiple intestinal neoplasia

MMR, Marc's modified Ringer's

MMTV, mouse mammary tumor virus

MSC, mesenchymal stem cell

MVEC, microvasculature endothelial cells

MyoFB, myofibroblast

NLK, Nemo-like kinase

OCT, Optimal Cutting Temperature compound

PAH, pulmonary arterial hypertension

PBS, phosphate buffered saline

PBST, phosphate buffered saline + Tween

PF, pulmonary fibrosis

PFA, paraformaldehyde

PH, pulmonary hypertension

PI4KIIa, phosphatidylinositol 4-kinase type IIa

PIP2, phosphatidylinositol (4,5)bis-phosphate

PIP5KI, phosphatidylinositol-4-phosphate 5-kinase type I

poly-ADP, adenosine diphosphate

PORCN, porcupine

Pygo, Pygopus

qPCR, quantitative polymerase change reaction

RSPOs, R-spondins

RTK, receptor tyrosine kinase

RVSP, right ventricular systolic pressure

SBE, Smad binding element

sFRPs, secreted Frizzled-related proteins

SMA, smooth muscle actin

TBS, tris-buffered saline

WIF-1, Wnt inhibitory factor 1

CHAPTER I: INTRODUCTION TO THE WNT SIGNALING PATHWAY

History of developmental biology: the question of form

"That which is formed by means of a process must of necessity be formed (a) out of something (b) by something (c) into something."

-Aristotle, *Generation of Animals* (Aristotle & Drossaart Lulofs, 1965)

To look at nature is to question it. How does an acorn grow into an oak? How does an adult grow from an infant? How does one organism with complex cellular architecture emerge from a single cell? While this thesis is concerned with Wnt signaling's role in disease and novel regulators for the pathway, these studies are built on data generated in pursuit of the ancient question: how does a being get its form? Aristotle addressed the question of form through examination of animals in the Island of Lesbos and summarized the common hypotheses of that time (roughly 340 BCE): that embryos contained all adult structures pre-formed ("preformation"), or that structures were unformed in the embryo and developed gradually ("epigenesis"). Aristotle favored epigenesis as he recognized that parts of various embryos developed successively but lacked the tools to explore this in detail. Robert Hooke's use of a microscope to study insects and plants in the 17th century provided early means to study biological mechanisms in detail and led to the first description of a cell. In his landmark work *Micrographia,* Hooke observed honey-comb like structures in a slice of magnified cork (Hooke, 1667). Matthias Schleiden and Theodore Schwann capitalized on microscopic examinations of both plant and animal cells in the 19th century to generate cell theory, stating in 1839 that all living things are composed of cells and that cells are the basic

unit of structure in organisms (Schwann, Smith, & Schleiden, 1847). Rudolf Virchow completed this statement with the concept that every cell arises from another cell (Virchow, 1858). The identification of the cell provided a backdrop for Hilde Mangold and Hans Spemann in the early 20th century to address Aristotle's question of preformation versus epigenesis (Spemann & Mangold, 2001). Mangold discovered that transplantation of the dorsal lip of one pigmented newt embryo to the ventral portion another embryo induced a secondary body axis (Spemann & Mangold, 2001). Importantly, because of pigmentation differences, Mangold was able to lineage trace the tissue of the secondary axis and found that it was mainly tissue from the recipient animal (Spemann & Mangold, 2001). Mangold concluded that the dorsal lip of the donor animal provided "organizing" compounds to the ventral embryonic tissue, implying that the embryo formed through a series of inductive events initiated by neighboring cells rather than existing as immutable elements (preformation) – agreeing with Aristotle's initial conclusion (Spemann & Mangold, 2001). While Mangold and Spemann theorized that inductive compounds were present, they were unable to identify them (Spemann & Mangold, 2001). Almost 50 years later, evidence of Mangold's and Spemann's compounds emerged through studies into oncogenes, or mutated forms of cellular genes. Many of these oncogenes encoded growth factors that provided framework into studies of both inter and intra-cellular communication (Hynes et al., 2013).

Signal transduction pathways

Cellular communication is required for a cell's response to physical stimuli. Cells have evolved a variety of different mechanisms to perceive their environment and respond to it, and almost all of these mechanisms are variations on a common theme. A

protein receptor at the cell membrane detects a physical stimulus, an initial messenger molecule transduces the stimulus signal from the receptor and amplifies this signal, and a second messenger receives the stimulus signal and initiates the cell's response (Gerhart, 1999; Pollard, Earnshaw, & Lippincott-Schwartz, 2008). The interaction route by which a signal is transduced from the physical stimulus to cellular response is known as a signaling transduction pathway. Despite the vast differences in metazoans, only 17 signal transduction pathways are believed to be responsible for much of cellular behavior, many of which likely emerged in pre-Cambrian times and only five of which are related to early development: receptor tyrosine kinase (RTK), Hedgehog, Notch, TGFβ, and Wnt (Gerhart, 1999). While the basic strategy of these mechanisms to transduce a signal from the membrane to its appropriate cellular response is similar, there are several different approaches that these pathways adopt. After ligand binding, some pathways activate a variety of messengers that in turn activate a series of protein kinases, as in the case of the RTK pathway. Some signaling pathways activate messengers which must be proteolytically cleaved before further pathway activation, as in the case of Hedgehog or Notch signaling. Some pathways simply activate a cytoplasmic messenger that translocates to the nucleus to initiate transcription, as in the case of TGFβ (Gerhart, 1999). Finally, some pathways actively degrade their messengers until a ligand binding to a receptor prevents this degradation, as in the case of Wnt signaling (Gerhart, 1999). Wnt and TGFβ signaling will be now discussed in greater detail.

Flies, frogs, and mice: the origins of Wnt signaling

While we are still identifying components of Wnt signaling, many of the core components of the pathway were identified using the integration of studies of model organisms in three separate biological disciplines: cancer studies in mice, genetic screens in flies, and developmental biology studies in frogs (Nusse & Varmus, 2012). The identification of the first ligand of the pathway, Wnt1, is a case study for this multidisciplinary approach. Taking advantage of the capacity of the mouse mammary tumor virus (MMTV) to deregulate nearby genes upon proviral insertion into the host genome, investigators Roel Nusse and Harold Varmus screened mammary tumors from mice infected with milk-borne MMTV (Nusse & Varmus, 2012). Out of this screen, one tumor contained a single proviral integration adjacent to a potential oncogene the investigators labelled *int-1* (Nusse & Varmus, 2012). Subsequent studies showed that transgenic mice carrying an MMTV long terminal repeat (LTR) upstream of the *int-1* gene develop mammary and salivary adenocarcinomas, establishing *int-1* as a potential proto-oncogene (Tsukamoto, Grosschedl, Guzman, Parslow, & Varmus, 1988). The *int-1* gene was shown to be evolutionarily conserved, and cDNA probes generated from *int-1* hybridized with a known fly gene, *wingless,* responsible for wing development (Rijsewijk et al., 1987). This identification was significant because it was the first instance of an oncogene being linked to known developmental mutants in *Drosophila* and provided evidence for theories that oncogenes were linked to development (Bishop, 1983). The identification of *wingless* as a developmental gene was possible due to the Nobel-prize winning work of Edward Lewis, Christiane Nusslein-Volhard, and Eric Wieschaus (Nusslein-Volhard & Wieschaus, 1980). Nusslein-Volhard's and Eric Wieschaus's study of segmentation and polarity defects in Drosophila larval screens

allowed biologists to identify the genetic mechanisms of development in a pre-cloning world. Nusslein-Volhard and Wieschaus confirmed known mutants, such as *wingless*, as well as identifying many novel phenotypes, such as *hedgehog* (Nusslein-Volhard & Wieschaus, 1980; Sharma & Chopra, 1976). The first biological assay for the developmental role of *int1* was performed by Andrew McMahon and Randell Moon, who found that *int1* mRNA injection caused axis duplication in *Xenopus leavis* embryos, confirming *int1*'s role in vertebrate dorsal mesoderm formation as well as invertebrate development (McMahon & Moon, 1989). *int1*'s ability to form a supernumerary axis also makes this protein the potential "organizing" molecule predicted by Spemann and Mangold 60 years earlier (McMahon & Moon, 1989). On the basis of this homology with the fly *wingless* gene, the initial name, *int-1,* was later changed to *Wnt1.* Subsequent studies using the same approach in MMTV mice identified two additional members of the Wnt family, Wnt-3 and Wnt-10b (Roelink, Wagenaar, Lopes da Silva, & Nusse, 1990). A number of other core components of the Wnt pathway were identified in fly mutant screens and confirmed using the *Xenopus laevis* duplication assay (Table 1).

Current model of Wnt signaling

The current model of Wnt signaling incorporates the core components discussed above as well as proteins responsible for Wnt ligand secretion, co-receptors, secreted modulators of Wnt signaling, and transcription factors (Figure 1). Activation of Wnt signaling transcription is dependent on the transcriptional co-activator, β-catenin. In the absence of a Wnt ligand, β-catenin is phosphorylated within a protein complex (destruction complex) consisting of the scaffolding proteins adenomatous polyposis coli (APC) and Axin and the kinases CK1α and GSK3 (reviewed in Saito-Diaz *et al*., 2013).

Axin serves as the rate-limiting component of the destruction complex (Salic, Lee, Mayer, & Kirschner, 2000). Its level is controlled by the poly-ADP (adenosine diphosphate)-ribose polymerase, tankyrase, that modifies Axin by poly-ADP-ribosylation (PARsylation), thereby targeting it for ubiquitination and proteasomal degradation. There are 19 mammalian Wnt variants that are all palmitoylated in the endoplasmic reticulum (ER) by the O-acetyltransferase protein, porcupine (PORCN). Palmitoylation is an essential modification that allows Wnt ligands to exit the ER and bind Frizzled (Fzd) receptors. Wnt ligands are also regulated by a variety of secreted inhibitors such as secreted Frizzled-related proteins (sFRPs) and Wnt inhibitory factor 1 (WIF-1). Upon binding of a Wnt ligand to the co-receptors LRP5/6 and Fzd, and in coordination with the action of cytoplasmic Dvl proteins, a Wnt signalosome complex is formed that consists of LRP6, Fzd and components of the β-catenin degradation complex. The current model proposes that phosphorylation (in part by the action of GSK3) of the intracellular domain of LRP5/6 generates a dock for the degradation complex. Within the signalosome, β-catenin phosphorylation by GSK3 is inhibited, thereby blocking its degradation and increasing its cytoplasmic levels. β-catenin ultimately translocates to the nucleus where it binds to TCF/LEF transcription factors (as well as a host of other nuclear factors, including Pygopus (Pygo), BCL9 and p300/CBP), to initiate a Wnt-specific transcriptional program that results, in many cases, in growth and proliferation. The levels of both Fzd (of which there are 10 mammalian variants) and LRP5/6 are regulated by the transmembrane E3 ligases, RNF43 and ZNRF3, which target them for ubiquitin-mediated degradation (Saito-Diaz et al., 2013). The activities of RNF43 and ZNRF3 are regulated by the R-spondins (RSPOs), secreted proteins that form a

complex with the seven transmembrane domain protein, Lgr5, to directly bind RNF43 and ZNRF3, blocking their activities.

Why study Wnt: Wnt signaling in organogenesis, stem cell maintenance and disease

Wnt signaling regulates stem cell maintenance, cancer development and fibrosis. Wnt signals act as self renewal factors for intestinal stem cells (Barker et al., 2007; Fevr, Robine, Louvard, & Huelsken, 2007; Korinek et al., 1998; van Es et al., 2012). Both TCF4 and β-catenin expression in intestinal epithelium are required for murine intestinal crypt homeostasis and genetic ablation of these components causes a rapid loss of crypt structure due to differentiation of stem cells located at the crypt-base (Fevr et al., 2007; Korinek et al., 1998; van Es et al., 2012). As blocking Wnt secretion in intestinal epithelial cells does not alter homeostasis, Wnt signaling at the crypt base is likely the result of local Wnt ligands secreted by the underlying intestinal mesenchyme (Kabiri et al., 2014; San Roman, Jayewickreme, Murtaugh, & Shivdasani, 2014; Valenta et al., 2016). Thus, localized Wnt ligand secretion may confer a “positional privilege” on nearby cell populations, establishing the stem cell niche (Clevers, Loh, & Nusse, 2014). The direction of Wnt ligands also dictate stem cell orientation during stem cell division- the cell farthest from the Wnt signal becomes the daughter cell that will differentiate as it migrates away from the Wnt ligand gradient (Habib et al., 2013; Yamashita, Jones, & Fuller, 2003). This data shows that Wnt ligands act as powerful morphogens in a highly localized fashion. The short range activity of Wnt signaling is likely due to two essential palmitoyl groups found on Wnt ligands which confer hydrophobicity to Wnt proteins. Surprisingly, flies generated with a mutant form of membrane-tethered Wingless show

no gross differences in morphology, implying that long range signaling is dispensable for Wnt induced developmental effects in *Drosophilia*. Membrane-tethered Wingless in this study only induced expression of Wnt target genes within several cells distance as opposed to across a gradient, confirming that other mechanisms of Wnt transport (transcytosis or exosomes) were not present in these mutants (Alexandre, Baena-Lopez, & Vincent, 2014; Janda, Waghray, Levin, Thomas, & Garcia, 2012).

While decreased expression of Wnt signaling components causes loss of intestinal stem cells, mutations of these components can lead to cancer in humans (Figure 1). APC is a component of the β-catenin destruction complex that has been the most frequently implicated in carcinogenesis. Clues as to the identification of the *APC* gene as a tumor suppressor in humans were first provided by a case study of a 42-year-old individual with developmental defects, large numbers of colon adenomatous polyps and a partial deletion of chromosome 5 (Herrera, Kakati, Gibas, Pietrzak, & Sandberg, 1986; Su et al., 1992). Soon afterwards, a mouse model that recapitulated the phenotype of familial adenomatous polyposis (FAP), an autosomal dominant disease characterized by high levels of colorectal adenomas, was generated through an *N*-ethyl-*N-nitrosourea* (ENU)-based forward genetic screen in mice (Su et al., 1992). The APC (Min/+) mouse (multiple intestinal neoplasia) features a premature stop codon at codon 850 of the APC sequence, yielding a truncated form of APC. Analysis of 224 colorectal human tumor samples showed that roughly 80% of CRC tumors contain mutations in APC (Cancer Genome Atlas, 2012). The majority of these somatic mutations (~60%) lie within a region near the middle of the APC protein known as the mutation cluster region (MCR). Because a series of 20 amino acid repeats known to bind β-catenin cluster

around the MCR, the current hypothesis for the mechanism of APC mutation-induced carcinogenesis is that APC acts as a tumor suppressor that, upon truncation, loses its capacity to bind β-catenin and target it for degradation (Aoki & Taketo, 2007; Fearnhead, Britton, & Bodmer, 2001). β-catenin is a transcriptional co-activator in the Wnt pathway that has both signaling and structural capabilities. It is composed of an *N*- and *C*-terminal domain flanking 12 centralized Armadillo (ARM) repeats that serve as binding regions for a variety of interacting proteins at the membrane and in the nucleus. Its levels are tightly regulated in the cytoplasm through a series of phosphorylation events that occur at serine/threonine sites encoded by exon 3 of *CTNNB1* (gene that codes for β-catenin) that mediate its turnover and maintain its low cytoplasmic levels. Missense mutations that alter these serine/threonine sites have been identified in colon and liver cancers (Austinat et al., 2008; Cancer Genome Atlas, 2012). In certain cancers, mutations in β-catenin are the predominant mutation in the Wnt pathway. Mutations in β-catenin accounts for only 5% of CRC (Cancer Genome Atlas, 2012). The prevalence of APC mutations in CRC is approximately 80% (Cancer Genome Atlas, 2012). The reason for these differences in prevalence in β-catenin and APC mutations in different organs is not clear. Axin is another component of the destruction complex and loss-of-function mutations of Axin are also associated with human cancers (Satoh *et al*., 2000; Muto *et al*., 2014). Several hepatocellular carcinoma cell lines (SNU423, SNU475 and Alexander) contain truncating mutations in Axin1; in several cell lines, Axin1 overexpression was more effective than APC overexpression in mediating suppression of TCF4 transcription (Satoh *et al*., 2000). Axin exists in two forms: Axin1 is constitutively expressed, whereas Axin2 is a Wnt target gene that is likely involved in

negative pathway feedback. Axin2 mutations are frequently frame-shift mutations leading to premature stop codons in exon 7, whereas Axin1 mutations are more evenly distributed throughout the protein (Taniguchi *et al*., 2005; Kim *et al*., 2009). Hypermethylation of Axin2 has been identified in adenomas from patients and the cancer cell line HCT116 (Muto *et al*., 2014). An emerging major mode of regulation for Wnt signaling at the membrane has been shown to occur between the co-receptors LRP5/6 and Fzd, and the transmembrane RING-type E3 ligases, ZNRF3 and RNF43. The targeting of Fzd receptors for ubiquitination and turnover by ZNRF3/RNF43 reduces the over-all responsiveness to Wnt proteins by decreasing the number of available receptors for pathway activation (Saito-Diaz *et al*., 2013). Early studies indicated that ZNRF/RNF43 act as negative regulators of Wnt signaling, implying that *ZNRF/RNF43* are potential tumor suppressors; in support of this model, homozygous deletion of *ZNRF/RNF43* in intestinal epithelium was found to induce adenomas in mice (Saito-Diaz *et al*., 2013). In studies of human colorectal tissue, a high number (18.9%) of samples displayed mutations in *ZNRF/*RNF43 (Giannakis *et al*., 2014). Similarly, high rates of *ZNRF/RNF43* mutations were found in endometrial and gastric cancer (18.1% and 8.1%, respectively) (Giannakis *et al*., 2014). Recently, the Clevers lab (Hubrecht Institute) generated a three-dimensional intestinal epithelial organoid derived from CRC tissue that contained an *RNF43* frameshift mutation and demonstrated that these organoids respond to small molecule inhibition of PORCN (van de Wetering *et al*., 2015). On the basis of these studies, a ‘living organoid biobank’ has been proposed as a strategy to develop personalised therapy for CRC (van de Wetering *et al*., 2015). RSPOs represent a family of secreted agonists of the Wnt pathway that form a trimeric

complex with ZNRF/RNF43 and LGR5. This trimeric complex inhibits ZNRF/RNF43-mediated ubiquitination of Fzd, thus potentiating Wnt signaling (Saito-Diaz *et al*., 2013). The important role of RSPO in maintaining normal intestinal homeostasis is demonstrated by the fact that fusions in RSPO have been found in 4–10% of CRC tumors (Seshagiri *et al*., 2012; Shinmura *et al*., 2014).

In addition to cancer, Wnt signaling represents a pathway that may activate developmental pathway re-engagement during fibrosis in a variety of tissues, including the adult lung. The lung develops from primitive foregut endoderm and Wnt signaling components are highly expressed during this early stage (Mucenski et al., 2003). Wnt signaling is required for the establishment of respiratory progenitors in the foregut and Wnt2/2b and Wnt7b are required for the formation of lung epithelial and mesenchymal structure during development (Goss et al., 2009). During development, the lung undergoes a process known as branching morphogenesis where lung epithelium grows into the fully formed bronchial tree. Nuclear β-catenin expression occurs early in budding alveolar structures and then declines. However, in a progressive fibrotic lung disorder known as idiopathic pulmonary fibrosis (IPF) nuclear β-catenin expression occurs in hyperplastic basal cells and fibrotic structures known as fibroblastic foci (Chilosi et al., 2003; Lam et al., 2014). These foci may represent areas of remodeling in the lung caused by re-induction of developmental Wnt ligands that cause dedifferentiation of nearby cells. These cells then differentiate to profibrotic lineages in a disease environment.

Wnt signaling cross talk

Given that Wnt signaling is active during development and disease, it is important

to observe how other signaling pathways interact with it. Cell signaling is a dynamic, context dependent process often determined by how multiple signaling pathways interact with each other, a process known as crosstalk. I will focus on the crosstalk between Wnt, Hedgehog and TGFβ signaling pathways as crosstalk between these pathways provide two examples of crosstalk mechanisms: direct interaction between pathway components and one pathway's effect on the expression of another pathway's core signaling components (Akhmetshina et al., 2012; Nusse, 2003). Wnt and Hedgehog were both identified as segment polarity genes (Nusslein-Volhard & Wieschaus, 1980). The ligands for both pathways, Wingless and Hedgehog, are palmitoylated, secreted, and bind to seven-transmembrane domain receptors (Nusse, 2003; Song et al., 2015). Both pathways have a messenger, Gli1 for Hedgehog or β-catenin for Wnt, that are targeted for degradation by GSK3 and CK1α. Phosphorylation of Gli1 causes the formation of a negative regulator of the Hedgehog pathway known as GliR which can also prevent the translocation of β-catenin to the nucleus. Gli1 also serves as a transcription factor for several regulators of Wnt signaling, such as Snail, Wnt, and sFRP1 (Song et al., 2015).

Like Wnt, the core components of the TGFβ pathway were identified through studies into cancer and developmental biology. TGFβ ligands were initially discovered when murine sarcoma virus-transformed mouse fibroblasts were found to form progressively growing colonies in soft agar (Todaro & De Larco, 1978). The factor responsible for this anchorage–independent growth was purified by several different labs and called "transforming growth factor" based on this growth ability (Moses, Branum, Proper, & Robinson, 1981; Roberts, Anzano, Lamb, Smith, & Sporn, 1981).

Early researchers were surprised that this new factor was not cancer specific and could be isolated from non-neoplastic tissues, suggesting TGFβ played a role in a variety of biological processes (Roberts et al., 1981). TGFβ receptors were identified through affinity cross-linking receptors with purified TGFβ (Frolik, Wakefield, Smith, & Sporn, 1984; Massague, Czech, Iwata, DeLarco, & Todaro, 1982; Massague & Like, 1985; Tucker, Branum, Shipley, Ryan, & Moses, 1984). Cytoplasmic components of the TGFβ pathway were found through *Drosophila* genetic screens attempting to isolate mutations that if present in the mother exacerbated decapentaplegic (dpp) phenotypes (Raftery, Twombly, Wharton, & Gelbart, 1995; Sekelsky, Newfeld, Raftery, Chartoff, & Gelbart, 1995). This screen identified proteins that were required for dpp function, which is a *Drosophila* morphogen that is part of the TGFβ family. Since these mutants were identified through a maternal screen, one of the mutants identified was unfortunately called Mothers against decapentaplegic (Mad) as a play on the name of the anti-drunk driving group, Mothers Against Drunk Driving (MADD). Similar studies in *C. elegans* identified the mammalian homologs of Mad known as Sma for small body size (Savage et al., 1996). To simplify nomenclature of a rapidly emerging field, the mammalian homolog of Mad became Smad, as a fusion of Mad and Sma (Derynck et al., 1996). Unlike β-catenin, Smads bind directly to DNA in a specific sequence known as a "Smad binding element" (SBE) to initiate transcription of TGFβ target genes (Shi & Massague, 2003).

Many studies have identified crosstalk between the nuclear components of the Wnt and TGFβ pathways (Crease, Dyson, & Gurdon, 1998; Cui, Tian, & Christian, 1996; Hussein, Duff, & Sirard, 2003; Labbe, Letamendia, & Attisano, 2000; Nishita et al.,

2000; Szeto & Kimelman, 2004). In *Xenopus,* Smad2 interacts with β-catenin to induce *Siamois* expression (Crease et al., 1998). Smad3 physically interacts with the HMG box domain of Lef1 to synergize transcription of *Xtwin* (Labbe et al., 2000; Nishita et al., 2000). Likewise, Lef1/Smad4 bind to synergistically activate Msx2 (Hussein et al., 2003). During fibrosis, crosstalk occurs as the key messenger for TGFβ, Smad, binds to the promoter for αSMA along with β-catenin. These studies demonstrate that the transcriptional complex of β-catenin/Tcf/Lef/Smad is common in many developmental as well as fibrotic-associated genes (Figure 2). Finally, many fibrotic diseases feature co-activation of both Wnt and TGFβ signaling (Akhmetshina et al., 2012).

Kinases in Wnt signaling

Wnt signaling is regulated through phosphorylation, a process where the γ-phosphatase of an ATP molecule is transferred to the hydroxyl-group of serine, threonine, or tyrosine on a protein (Verheyen & Gottardi, 2010). This chemical reaction is catalyzed by a class of enzymes known as kinases, one of the largest classes of proteins; protein kinase domains are found in 2% of eukaryotic genes (Verheyen & Gottardi, 2010). Kinases consist of a two-lobed structure with an ATP-binding cleft located between the lobes. Many kinases contain an activation loop that when phosphorylated stabilizes the kinase in a conformation available for substrate binding (Verheyen & Gottardi, 2010). Wnt signaling regulation by kinases remains an intense area of research, and currently there are five kinases that have been identified whose activities have a direct effect on Wnt signaling: GSK3, CK1, PIP5KI, HIPK, and NLK. While PIP5KI operates at the level of the membrane and HIPK/NLK operate at the

nucleus, CK1 and GSK3 phosphorylate substrates at the membrane, cytoplasm and nucleus (Verheyen & Gottardi, 2010).

GSK3 (or *Drosophila* zeste white/shaggy) was originally identified as a serine/threonine kinase that acts as a negative regulator of β-catenin (*Drosophila* armadillo) (Bourouis et al., 1990; Siegfried, Perkins, Capaci, & Perrimon, 1990). GSK3 not only phosphorylates β-catenin but also Axin, which when phosphorylated promotes β-catenin binding to the destruction complex (Jho, Lomvardas, & Costantini, 1999; Luo et al., 2007; Willert, Shibamoto, & Nusse, 1999). GSK3 was also found to phosphorylate the intracellular domain of LRP6, allowing the cytoplasmic portion of LRP6 to serve as a docking site for Axin upon Wnt ligand binding (Pinson, Brennan, Monkley, Avery, & Skarnes, 2000; Tamai et al., 2000; Tamai et al., 2004; Wehrli et al., 2000). GSK3 phosphorylates the cytoplasmic tail of LRP6 at PPPSP sites, which serves as a priming event for subsequent CK1γ phosphorylation (Bilic et al., 2007; Davidson et al., 2005; Zeng et al., 2008; Zeng et al., 2005). Importantly, Axin association with the ICD of LRP6 is a key initial step for inactivation of the destruction complex. Thus, GSK3 plays a dual regulatory role for the Wnt pathway-GSK3 phosphorylation of LRP6 induces activation of the pathway and GSK3 phosphorylation of Axin and β-catenin causes pathway inhibition (Zeng et al., 2005). Interestingly, LRP6 can directly inhibit GSK3 kinase activity (Cselenyi et al., 2008; Piao et al., 2008). Recent evidence also shows that Wnt activation inhibits GSK3 activity via a mechanism involving multivesicular GSK3 sequestration (Vinyoles et al., 2014). To add an additional layer of complexity of the role of GSK3 in Wnt signaling, GSK3 also binds and phosphorylates the transcription factor TCF3, decreasing transcription of Wnt target genes (E. Lee, Salic, & Kirschner, 2001).

The activity of GSK3 occurs in concert with the activity of CK1 (*Drosophila* Gilgamesh) in the Wnt pathway. GSK3 primes CK1γ LRP6 phosphorylation whereas CK1α primes GSK3 phosphorylation of β-catenin (Bilic et al., 2007; Davidson et al., 2005; Zeng et al., 2008; Zeng et al., 2005). CK1 also phosphorylates TCF3, increasing transcription of Wnt target genes and may promote phosphorylated TCF3 to inhibit β-catenin degradation (E. Lee et al., 2001). CK1 plays an important role in Wnt activation by phosphorylating the cytosolic protein Dishevelled (Dsh or Dvl) (J. S. Lee, Ishimoto, & Yanagawa, 1999; Rothbacher et al., 2000; Willert et al., 1999). Dvl is required for Wnt signaling transduction, and Dvl aggregates are formed after Wnt ligand stimulation (Wehrli et al., 2000; Zeng et al., 2008). Dvl interacts with Fzd and acts as a membrane localized platform for Axin and GSK3 (J. S. Lee et al., 1999; Rothbacher et al., 2000; Willert et al., 1999).

In an siRNA screen to uncover novel kinases targeting LRP6, investigators identified phosphatidylinositol 4-kinase type IIa (PI4KIIa) and phosphatidylinositol-4-phosphate 5-kinase type I (PIP5KI), two kinases that generate phosphatidylinositol (4,5)bis-phosphate (PIP2) (Pan et al., 2008). PI4KIIa and PIP5KI were shown to be required for β-catenin accumulation, LRP6 phosphorylation and promoted axis duplication in *Xenopus* embryos. Dvl was found to be required for the activity of PI4KIIa and PIP5KI in the Wnt pathway. Sucrose density gradient ultracentrifugation demonstrated that PIP2 is present in membrane fractions containing LRP6 and increased after Wnt3a treatment. Based on these studies, a model was proposed in which upon Wnt ligand binding, Dvl associates with Fz and activates PI4KIIa and PIP5KI, which in turn induce aggregation of the LRP6 signalosome (Pan et al., 2008).

Similar to CK1 and GSK3, PI4KIIa and PIP5KI regulate the Wnt signaling pathway through interactions with Wnt receptors.

Nemo-like kinase (NLK) and homeodomain-interacting protein kinase (HIPK) are two kinases that have been shown to target the transcription factor TCF (Verheyen & Gottardi, 2010). NLK is related to MAP-kinases and acts as a negative regulator of Wnt signaling. NLK overexpression suppresses β-catenin accumulation in cultured cells and inhibits axis duplication in *Xenopus* embryos (Ishitani et al., 1999). Phosphorylation of TCF by NLK blocks β-catenin/TCF formation, preventing transcription (Ishitani et al., 1999). NLK has also been shown to bind Dvl, although the significance of this interaction is not clear (Ota et al., 2012). HIPK is a positive regulator of the Wnt pathway that rescues loss of Wingless in flies, binds and stabilizes Arm, and promotes TOPFLASH activity (Verheyen & Gottardi, 2010). Acting in a similar fashion to NKL, HIPK inhibits the Wnt pathway by phosphorylating TCF3, promoting the disassociation of TCF3 from a target promoter and the binding of the initiating transcription factor TCF1 (Hikasa & Sokol, 2011). Although NLK and HIPK both target TCF, they have opposing activities, illustrating the dynamic nature of Wnt pathway regulation by phosphorylation. Finally, by binding to nuclear as well as cytoplasmic components, NLK and HIPK act in a similar manner as CK1 and GSK3 in targeting multiple substrates in the Wnt pathway.

Mammalian	Fly
Wnt1	Wingless
GSK3	Shaggy/Zeste-white 3
β-catenin	Armadillo
Axin	Fused
Frizzled	Frizzled
LRP6	Arrow
TCF	Pangolin
Dishevelled	Dishevelled
TLE	Groucho

Table 1: Wnt signaling genes in mammals and orthologs in *Drosophilia*.

Figure 1

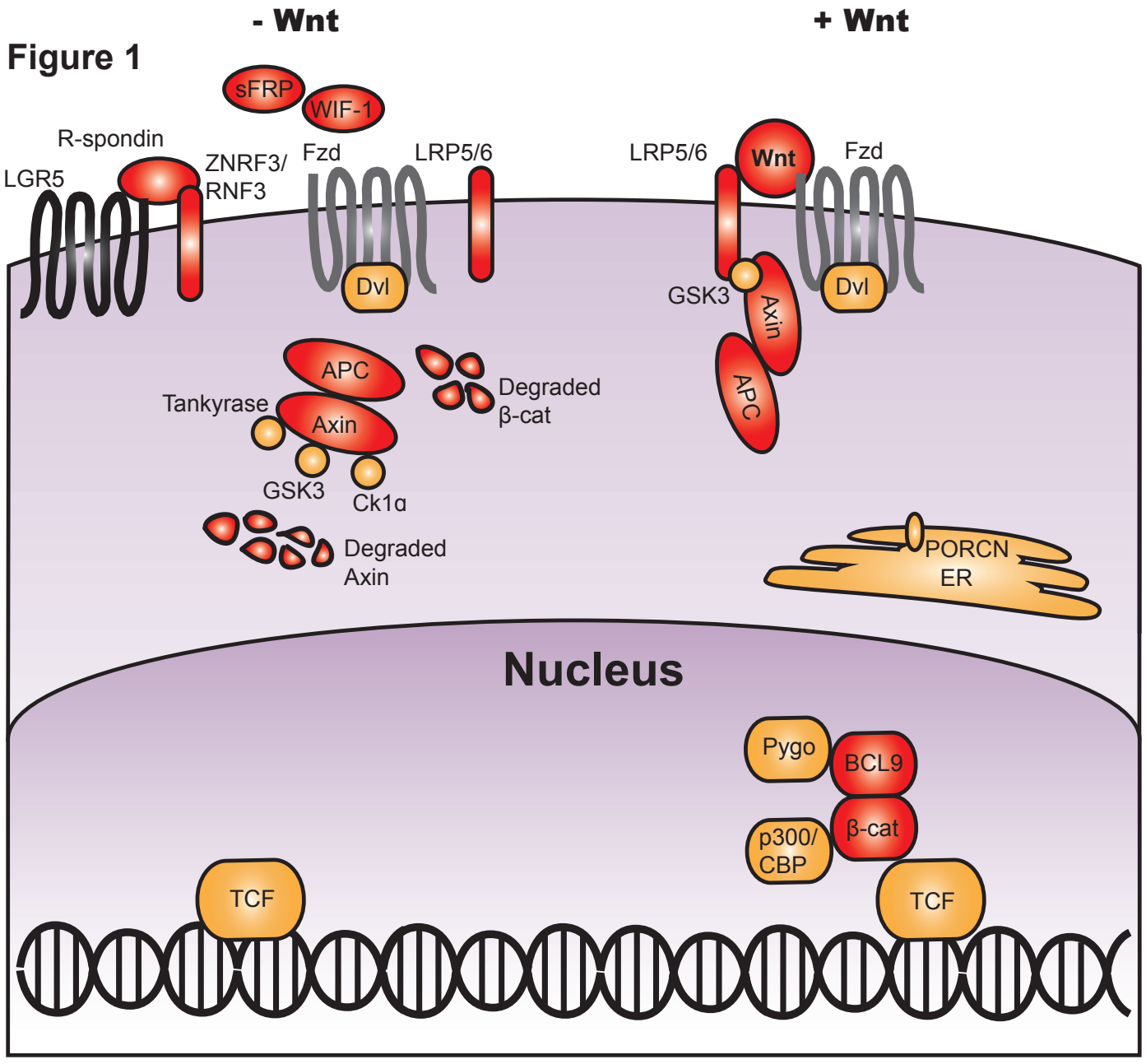

Figure 1: Current model of Wnt signal transduction. Wnt components known to be altered in human cancers are shown in red. Details in text.

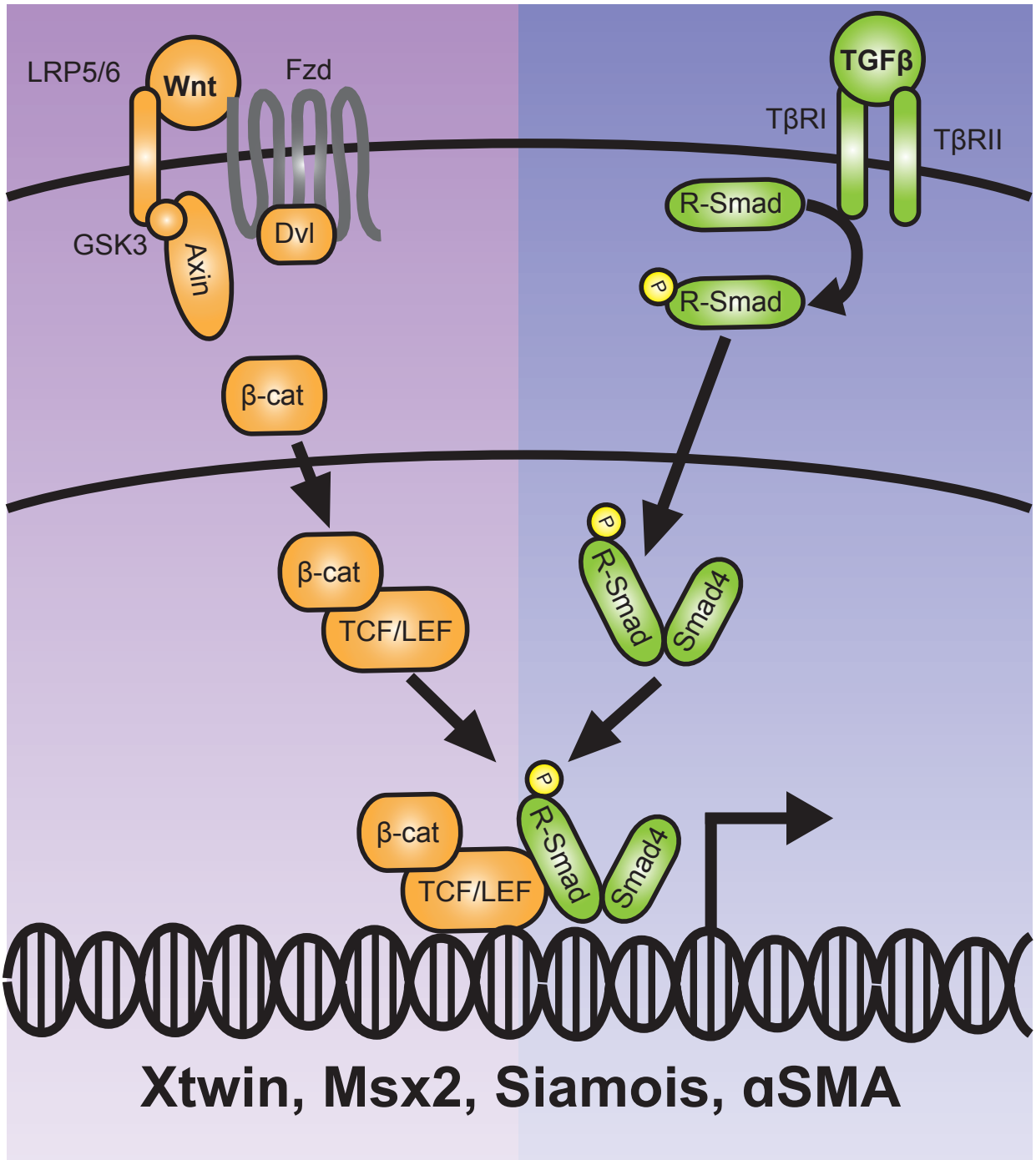

Figure 2: Crosstalk between Wnt and TGFβ pathways. Details in text.

References

Akhmetshina, A., Palumbo, K., Dees, C., Bergmann, C., Venalis, P., Zerr, P., . . . Distler, J. H. (2012). Activation of canonical Wnt signalling is required for TGFbeta-mediated fibrosis. *Nat Commun, 3*, 735. doi:10.1038/ncomms1734

Alexandre, C., Baena-Lopez, A., & Vincent, J. P. (2014). Patterning and growth control by membrane-tethered Wingless. *Nature, 505*(7482), 180-185. doi:10.1038/nature12879

Aoki, K., & Taketo, M. M. (2007). Adenomatous polyposis coli (APC): a multi-functional tumor suppressor gene. *J Cell Sci, 120*(Pt 19), 3327-3335. doi:10.1242/jcs.03485

Aristotle, & Drossaart Lulofs, H. J. (1965). *Aristotelis De generatione animalium*. Oxonii,: E Typographeo Clarendoniano.

Austinat, M., Dunsch, R., Wittekind, C., Tannapfel, A., Gebhardt, R., & Gaunitz, F. (2008). Correlation between beta-catenin mutations and expression of Wnt-signaling target genes in hepatocellular carcinoma. *Mol Cancer, 7*, 21. doi:10.1186/1476-4598-7-21

Barker, N., van Es, J. H., Kuipers, J., Kujala, P., van den Born, M., Cozijnsen, M., . . . Clevers, H. (2007). Identification of stem cells in small intestine and colon by marker gene Lgr5. *Nature, 449*(7165), 1003-1007. doi:10.1038/nature06196

Bilic, J., Huang, Y. L., Davidson, G., Zimmermann, T., Cruciat, C. M., Bienz, M., & Niehrs, C. (2007). Wnt induces LRP6 signalosomes and promotes dishevelled-dependent LRP6 phosphorylation. *Science, 316*(5831), 1619-1622. doi:10.1126/science.1137065

Bishop, J. M. (1983). Cellular oncogenes and retroviruses. *Annu Rev Biochem, 52*, 301-354. doi:10.1146/annurev.bi.52.070183.001505

Bourouis, M., Moore, P., Ruel, L., Grau, Y., Heitzler, P., & Simpson, P. (1990). An early embryonic product of the gene shaggy encodes a serine/threonine protein kinase related to the CDC28/cdc2+ subfamily. *EMBO J, 9*(9), 2877-2884.

Cancer Genome Atlas, N. (2012). Comprehensive molecular characterization of human colon and rectal cancer. *Nature, 487*(7407), 330-337. doi:10.1038/nature11252

Chilosi, M., Poletti, V., Zamo, A., Lestani, M., Montagna, L., Piccoli, P., . . . Doglioni, C. (2003). Aberrant Wnt/beta-catenin pathway activation in idiopathic pulmonary fibrosis. *Am J Pathol, 162*(5), 1495-1502.

Clevers, H., Loh, K. M., & Nusse, R. (2014). Stem cell signaling. An integral program for tissue renewal and regeneration: Wnt signaling and stem cell control. *Science, 346*(6205), 1248012. doi:10.1126/science.1248012

Crease, D. J., Dyson, S., & Gurdon, J. B. (1998). Cooperation between the activin and Wnt pathways in the spatial control of organizer gene expression. *Proc Natl Acad Sci U S A, 95*(8), 4398-4403.

Cselenyi, C. S., Jernigan, K. K., Tahinci, E., Thorne, C. A., Lee, L. A., & Lee, E. (2008). LRP6 transduces a canonical Wnt signal independently of Axin degradation by inhibiting GSK3's phosphorylation of beta-catenin. *Proc Natl Acad Sci U S A, 105*(23), 8032-8037. doi:10.1073/pnas.0803025105

Cui, Y., Tian, Q., & Christian, J. L. (1996). Synergistic effects of Vg1 and Wnt signals in the specification of dorsal mesoderm and endoderm. *Dev Biol, 180*(1), 22-34. doi:10.1006/dbio.1996.0281

Davidson, G., Wu, W., Shen, J., Bilic, J., Fenger, U., Stannek, P., . . . Niehrs, C. (2005). Casein kinase 1 gamma couples Wnt receptor activation to cytoplasmic signal transduction. *Nature, 438*(7069), 867-872. doi:10.1038/nature04170

Derynck, R., Gelbart, W. M., Harland, R. M., Heldin, C. H., Kern, S. E., Massague, J., . . . Wang, X. F. (1996). Nomenclature: vertebrate mediators of TGFbeta family signals. *Cell, 87*(2), 173.

Fearnhead, N. S., Britton, M. P., & Bodmer, W. F. (2001). The ABC of APC. *Hum Mol Genet, 10*(7), 721-733.

Fevr, T., Robine, S., Louvard, D., & Huelsken, J. (2007). Wnt/beta-catenin is essential for intestinal homeostasis and maintenance of intestinal stem cells. *Mol Cell Biol, 27*(21), 7551-7559. doi:10.1128/MCB.01034-07

Frolik, C. A., Wakefield, L. M., Smith, D. M., & Sporn, M. B. (1984). Characterization of a membrane receptor for transforming growth factor-beta in normal rat kidney fibroblasts. *J Biol Chem, 259*(17), 10995-11000.

Gerhart, J. (1999). 1998 Warkany lecture: signaling pathways in development. *Teratology, 60*(4), 226-239. doi:10.1002/(SICI)1096-9926(199910)60:4<226::AID-TERA7>3.0.CO;2-W

Goss, A. M., Tian, Y., Tsukiyama, T., Cohen, E. D., Zhou, D., Lu, M. M., . . . Morrisey, E. E. (2009). Wnt2/2b and beta-catenin signaling are necessary and sufficient to specify lung progenitors in the foregut. *Dev Cell, 17*(2), 290-298. doi:10.1016/j.devcel.2009.06.005

Habib, S. J., Chen, B. C., Tsai, F. C., Anastassiadis, K., Meyer, T., Betzig, E., & Nusse, R. (2013). A localized Wnt signal orients asymmetric stem cell division in vitro. *Science, 339*(6126), 1445-1448. doi:10.1126/science.1231077

Herrera, L., Kakati, S., Gibas, L., Pietrzak, E., & Sandberg, A. A. (1986). Gardner syndrome in a man with an interstitial deletion of 5q. *Am J Med Genet, 25*(3), 473-476. doi:10.1002/ajmg.1320250309

Hikasa, H., & Sokol, S. Y. (2011). Phosphorylation of TCF proteins by homeodomain-interacting protein kinase 2. *J Biol Chem, 286*(14), 12093-12100. doi:10.1074/jbc.M110.185280

Hooke, R. (1667). *Micrographia*. London,.

Hussein, S. M., Duff, E. K., & Sirard, C. (2003). Smad4 and beta-catenin co-activators functionally interact with lymphoid-enhancing factor to regulate graded expression of Msx2. *J Biol Chem, 278*(49), 48805-48814. doi:10.1074/jbc.M305472200

Hynes, N. E., Ingham, P. W., Lim, W. A., Marshall, C. J., Massague, J., & Pawson, T. (2013). Signalling change: signal transduction through the decades. *Nat Rev Mol Cell Biol, 14*(6), 393-398. doi:10.1038/nrm3581

Ishitani, T., Ninomiya-Tsuji, J., Nagai, S., Nishita, M., Meneghini, M., Barker, N., . . . Matsumoto, K. (1999). The TAK1-NLK-MAPK-related pathway antagonizes signalling between beta-catenin and transcription factor TCF. *Nature, 399*(6738), 798-802. doi:10.1038/21674

Janda, C. Y., Waghray, D., Levin, A. M., Thomas, C., & Garcia, K. C. (2012). Structural basis of Wnt recognition by Frizzled. *Science, 337*(6090), 59-64. doi:10.1126/science.1222879

Jho, E., Lomvardas, S., & Costantini, F. (1999). A GSK3beta phosphorylation site in axin modulates interaction with beta-catenin and Tcf-mediated gene expression. *Biochem Biophys Res Commun, 266*(1), 28-35. doi:10.1006/bbrc.1999.1760

Kabiri, Z., Greicius, G., Madan, B., Biechele, S., Zhong, Z., Zaribafzadeh, H., . . . Virshup, D. M. (2014). Stroma provides an intestinal stem cell niche in the absence of epithelial Wnts. *Development, 141*(11), 2206-2215. doi:10.1242/dev.104976

Korinek, V., Barker, N., Moerer, P., van Donselaar, E., Huls, G., Peters, P. J., & Clevers, H. (1998). Depletion of epithelial stem-cell compartments in the small intestine of mice lacking Tcf-4. *Nat Genet, 19*(4), 379-383. doi:10.1038/1270

Labbe, E., Letamendia, A., & Attisano, L. (2000). Association of Smads with lymphoid enhancer binding factor 1/T cell-specific factor mediates cooperative signaling by the transforming growth factor-beta and wnt pathways. *Proc Natl Acad Sci U S A, 97*(15), 8358-8363. doi:10.1073/pnas.150152697

Lam, A. P., Herazo-Maya, J. D., Sennello, J. A., Flozak, A. S., Russell, S., Mutlu, G. M., . . . Gottardi, C. J. (2014). Wnt coreceptor Lrp5 is a driver of idiopathic pulmonary fibrosis. *Am J Respir Crit Care Med, 190*(2), 185-195. doi:10.1164/rccm.201401-0079OC

Lee, E., Salic, A., & Kirschner, M. W. (2001). Physiological regulation of [beta]-catenin stability by Tcf3 and CK1epsilon. *J Cell Biol, 154*(5), 983-993. doi:10.1083/jcb.200102074

Lee, J. S., Ishimoto, A., & Yanagawa, S. (1999). Characterization of mouse dishevelled (Dvl) proteins in Wnt/Wingless signaling pathway. *J Biol Chem, 274*(30), 21464-21470.

Luo, W., Peterson, A., Garcia, B. A., Coombs, G., Kofahl, B., Heinrich, R., . . . Virshup, D. M. (2007). Protein phosphatase 1 regulates assembly and function of the beta-catenin degradation complex. *EMBO J, 26*(6), 1511-1521. doi:10.1038/sj.emboj.7601607

Massague, J., Czech, M. P., Iwata, K., DeLarco, J. E., & Todaro, G. J. (1982). Affinity labeling of a transforming growth factor receptor that does not interact with epidermal growth factor. *Proc Natl Acad Sci U S A, 79*(22), 6822-6826.

Massague, J., & Like, B. (1985). Cellular receptors for type beta transforming growth factor. Ligand binding and affinity labeling in human and rodent cell lines. *J Biol Chem, 260*(5), 2636-2645.

McMahon, A. P., & Moon, R. T. (1989). Ectopic expression of the proto-oncogene int-1 in Xenopus embryos leads to duplication of the embryonic axis. *Cell, 58*(6), 1075-1084.

Moses, H. L., Branum, E. L., Proper, J. A., & Robinson, R. A. (1981). Transforming growth factor production by chemically transformed cells. *Cancer Res, 41*(7), 2842-2848.

Mucenski, M. L., Wert, S. E., Nation, J. M., Loudy, D. E., Huelsken, J., Birchmeier, W., . . . Whitsett, J. A. (2003). beta-Catenin is required for specification of

proximal/distal cell fate during lung morphogenesis. *J Biol Chem, 278*(41), 40231-40238. doi:10.1074/jbc.M305892200
Nishita, M., Hashimoto, M. K., Ogata, S., Laurent, M. N., Ueno, N., Shibuya, H., & Cho, K. W. (2000). Interaction between Wnt and TGFbeta signalling pathways during formation of Spemann's organizer. *Nature, 403*(6771), 781-785. doi:10.1038/35001602
Nusse, R. (2003). Wnts and Hedgehogs: lipid-modified proteins and similarities in signaling mechanisms at the cell surface. *Development, 130*(22), 5297-5305. doi:10.1242/dev.00821
Nusse, R., & Varmus, H. (2012). Three decades of Wnts: a personal perspective on how a scientific field developed. *EMBO J, 31*(12), 2670-2684. doi:10.1038/emboj.2012.146
Nusslein-Volhard, C., & Wieschaus, E. (1980). Mutations affecting segment number and polarity in Drosophila. *Nature, 287*(5785), 795-801.
Ota, S., Ishitani, S., Shimizu, N., Matsumoto, K., Itoh, M., & Ishitani, T. (2012). NLK positively regulates Wnt/beta-catenin signalling by phosphorylating LEF1 in neural progenitor cells. *EMBO J, 31*(8), 1904-1915. doi:10.1038/emboj.2012.46
Pan, W., Choi, S. C., Wang, H., Qin, Y., Volpicelli-Daley, L., Swan, L., . . . Wu, D. (2008). Wnt3a-mediated formation of phosphatidylinositol 4,5-bisphosphate regulates LRP6 phosphorylation. *Science, 321*(5894), 1350-1353. doi:10.1126/science.1160741
Piao, S., Lee, S. H., Kim, H., Yum, S., Stamos, J. L., Xu, Y., . . . Ha, N. C. (2008). Direct inhibition of GSK3beta by the phosphorylated cytoplasmic domain of LRP6 in Wnt/beta-catenin signaling. *PLoS One, 3*(12), e4046. doi:10.1371/journal.pone.0004046
Pinson, K. I., Brennan, J., Monkley, S., Avery, B. J., & Skarnes, W. C. (2000). An LDL-receptor-related protein mediates Wnt signalling in mice. *Nature, 407*(6803), 535-538. doi:10.1038/35035124
Pollard, T. D., Earnshaw, W. C., & Lippincott-Schwartz, J. (2008). *Cell biology* (2nd ed.). Philadelphia: Saunders/Elsevier.
Raftery, L. A., Twombly, V., Wharton, K., & Gelbart, W. M. (1995). Genetic screens to identify elements of the decapentaplegic signaling pathway in Drosophila. *Genetics, 139*(1), 241-254.
Rijsewijk, F., Schuermann, M., Wagenaar, E., Parren, P., Weigel, D., & Nusse, R. (1987). The Drosophila homolog of the mouse mammary oncogene int-1 is identical to the segment polarity gene wingless. *Cell, 50*(4), 649-657.
Roberts, A. B., Anzano, M. A., Lamb, L. C., Smith, J. M., & Sporn, M. B. (1981). New class of transforming growth factors potentiated by epidermal growth factor: isolation from non-neoplastic tissues. *Proc Natl Acad Sci U S A, 78*(9), 5339-5343.
Roelink, H., Wagenaar, E., Lopes da Silva, S., & Nusse, R. (1990). Wnt-3, a gene activated by proviral insertion in mouse mammary tumors, is homologous to int-1/Wnt-1 and is normally expressed in mouse embryos and adult brain. *Proc Natl Acad Sci U S A, 87*(12), 4519-4523.
Rothbacher, U., Laurent, M. N., Deardorff, M. A., Klein, P. S., Cho, K. W., & Fraser, S. E. (2000). Dishevelled phosphorylation, subcellular localization and

multimerization regulate its role in early embryogenesis. *EMBO J, 19*(5), 1010-1022. doi:10.1093/emboj/19.5.1010
Saito-Diaz, K., Chen, T. W., Wang, X., Thorne, C. A., Wallace, H. A., Page-McCaw, A., & Lee, E. (2013). The way Wnt works: components and mechanism. *Growth Factors, 31*(1), 1-31. doi:10.3109/08977194.2012.752737
Salic, A., Lee, E., Mayer, L., & Kirschner, M. W. (2000). Control of beta-catenin stability: reconstitution of the cytoplasmic steps of the wnt pathway in Xenopus egg extracts. *Mol Cell, 5*(3), 523-532.
San Roman, A. K., Jayewickreme, C. D., Murtaugh, L. C., & Shivdasani, R. A. (2014). Wnt secretion from epithelial cells and subepithelial myofibroblasts is not required in the mouse intestinal stem cell niche in vivo. *Stem Cell Reports, 2*(2), 127-134. doi:10.1016/j.stemcr.2013.12.012
Savage, C., Das, P., Finelli, A. L., Townsend, S. R., Sun, C. Y., Baird, S. E., & Padgett, R. W. (1996). Caenorhabditis elegans genes sma-2, sma-3, and sma-4 define a conserved family of transforming growth factor beta pathway components. *Proc Natl Acad Sci U S A, 93*(2), 790-794.
Schwann, T., Smith, H., & Schleiden, M. J. (1847). *Microscopical researches into the accordance in the structure and growth of animals and plants*. London,: The Sydenham Society.
Sekelsky, J. J., Newfeld, S. J., Raftery, L. A., Chartoff, E. H., & Gelbart, W. M. (1995). Genetic characterization and cloning of mothers against dpp, a gene required for decapentaplegic function in Drosophila melanogaster. *Genetics, 139*(3), 1347-1358.
Sharma, R. P., & Chopra, V. L. (1976). Effect of the Wingless (wg1) mutation on wing and haltere development in Drosophila melanogaster. *Dev Biol, 48*(2), 461-465.
Shi, Y., & Massague, J. (2003). Mechanisms of TGFbeta signaling from cell membrane to the nucleus. *Cell, 113*(6), 685-700.
Siegfried, E., Perkins, L. A., Capaci, T. M., & Perrimon, N. (1990). Putative protein kinase product of the Drosophila segment-polarity gene zeste-white3. *Nature, 345*(6278), 825-829. doi:10.1038/345825a0
Song, W. J., Song, E. A., Jung, M. S., Choi, S. H., Baik, H. H., Jin, B. K., . . . Chung, S. H. (2015). Phosphorylation and inactivation of glycogen synthase kinase 3beta (GSK3beta) by dual-specificity tyrosine phosphorylation-regulated kinase 1A (Dyrk1A). *J Biol Chem, 290*(4), 2321-2333. doi:10.1074/jbc.M114.594952
Spemann, H., & Mangold, H. (2001). Induction of embryonic primordia by implantation of organizers from a different species. 1923. *Int J Dev Biol, 45*(1), 13-38.
Su, L. K., Kinzler, K. W., Vogelstein, B., Preisinger, A. C., Moser, A. R., Luongo, C., . . . Dove, W. F. (1992). Multiple intestinal neoplasia caused by a mutation in the murine homolog of the APC gene. *Science, 256*(5057), 668-670.
Szeto, D. P., & Kimelman, D. (2004). Combinatorial gene regulation by Bmp and Wnt in zebrafish posterior mesoderm formation. *Development, 131*(15), 3751-3760. doi:10.1242/dev.01236
Tamai, K., Semenov, M., Kato, Y., Spokony, R., Liu, C., Katsuyama, Y., . . . He, X. (2000). LDL-receptor-related proteins in Wnt signal transduction. *Nature, 407*(6803), 530-535. doi:10.1038/35035117

Tamai, K., Zeng, X., Liu, C., Zhang, X., Harada, Y., Chang, Z., & He, X. (2004). A mechanism for Wnt coreceptor activation. *Mol Cell, 13*(1), 149-156.

Todaro, G. J., & De Larco, J. E. (1978). Growth factors produced by sarcoma virus-transformed cells. *Cancer Res, 38*(11 Pt 2), 4147-4154.

Tsukamoto, A. S., Grosschedl, R., Guzman, R. C., Parslow, T., & Varmus, H. E. (1988). Expression of the int-1 gene in transgenic mice is associated with mammary gland hyperplasia and adenocarcinomas in male and female mice. *Cell, 55*(4), 619-625.

Tucker, R. F., Branum, E. L., Shipley, G. D., Ryan, R. J., & Moses, H. L. (1984). Specific binding to cultured cells of 125I-labeled type beta transforming growth factor from human platelets. *Proc Natl Acad Sci U S A, 81*(21), 6757-6761.

Valenta, T., Degirmenci, B., Moor, A. E., Herr, P., Zimmerli, D., Moor, M. B., . . . Basler, K. (2016). Wnt Ligands Secreted by Subepithelial Mesenchymal Cells Are Essential for the Survival of Intestinal Stem Cells and Gut Homeostasis. *Cell Rep, 15*(5), 911-918. doi:10.1016/j.celrep.2016.03.088

van Es, J. H., Haegebarth, A., Kujala, P., Itzkovitz, S., Koo, B. K., Boj, S. F., . . . Clevers, H. (2012). A critical role for the Wnt effector Tcf4 in adult intestinal homeostatic self-renewal. *Mol Cell Biol, 32*(10), 1918-1927. doi:10.1128/MCB.06288-11

Verheyen, E. M., & Gottardi, C. J. (2010). Regulation of Wnt/beta-catenin signaling by protein kinases. *Dev Dyn, 239*(1), 34-44. doi:10.1002/dvdy.22019

Vinyoles, M., Del Valle-Perez, B., Curto, J., Vinas-Castells, R., Alba-Castellon, L., Garcia de Herreros, A., & Dunach, M. (2014). Multivesicular GSK3 sequestration upon Wnt signaling is controlled by p120-catenin/cadherin interaction with LRP5/6. *Mol Cell, 53*(3), 444-457. doi:10.1016/j.molcel.2013.12.010

Virchow, R. (1858). *Die cellularpathologie in ihrer begründung auf physiologische und pathologische gewebelehre*. Berlin,: A. Hirschwald.

Wehrli, M., Dougan, S. T., Caldwell, K., O'Keefe, L., Schwartz, S., Vaizel-Ohayon, D., . . . DiNardo, S. (2000). arrow encodes an LDL-receptor-related protein essential for Wingless signalling. *Nature, 407*(6803), 527-530. doi:10.1038/35035110

Willert, K., Shibamoto, S., & Nusse, R. (1999). Wnt-induced dephosphorylation of axin releases beta-catenin from the axin complex. *Genes Dev, 13*(14), 1768-1773.

Yamashita, Y. M., Jones, D. L., & Fuller, M. T. (2003). Orientation of asymmetric stem cell division by the APC tumor suppressor and centrosome. *Science, 301*(5639), 1547-1550. doi:10.1126/science.1087795

Zeng, X., Huang, H., Tamai, K., Zhang, X., Harada, Y., Yokota, C., . . . He, X. (2008). Initiation of Wnt signaling: control of Wnt coreceptor Lrp6 phosphorylation/activation via frizzled, dishevelled and axin functions. *Development, 135*(2), 367-375. doi:10.1242/dev.013540

Zeng, X., Tamai, K., Doble, B., Li, S., Huang, H., Habas, R., . . . He, X. (2005). A dual-kinase mechanism for Wnt co-receptor phosphorylation and activation. *Nature, 438*(7069), 873-877. doi:10.1038/nature04185

CHAPTER II: TGFβ INDUCTION AFTER BLEOMYCIN LUNG INJURY INCREASES WNT SIGNALING IN ADULT LUNG MESENCYMAL STEM CELLS

Pulmonary fibrosis (PF) is remodeling of the lung characterized by mesenchymal expansion, excessive extracellular matrix (ECM) deposition that depletes areas of gas exchange (Noble, Barkauskas, & Jiang, 2012), and the appearance of a cell type known as a myofibroblast (MyoFB). Pulmonary hypertension (PH) is a devastating pulmonary disorder that is a consequence of many diseases including PF, a progressive and fatal scarring illness of the lung. The development of PH in PF substantially worsens prognosis and limits survival. PH is characterized by vascular remodeling, dysfunction and ultimately right heart failure. Parenchymal and vascular remodeling by mesenchymal-derived cells, such as MyoFBs, likely share mechanisms that may explain the prevalence of pulmonary hypertension in pulmonary fibrosis (PF) and other interstitial lung disease (ILD) patients. (Marriott et al., 2014; McNulty & Janes, 2012; Noble et al., 2012; Phan, 2012).

MyoFBs in PF contribute to pulmonary microvascular remodeling and represent one of the cellular sources that drive PH. The following cell types also differentiate to a MyoFB phenotype during lung injury: resident fibroblasts, epithelial cells, endothelial cells, pericytes, and bone marrow-derived mesenchymal cells (BM-MC) also known as fibrocytes (Phan, 2012; Scotton & Chambers, 2007). In addition, a novel mesenchymal stem cell (MSC) population identified by the expression of the ATP binding cassette sub-family G member 2 ($ABCG2^{pos}$) protein is another source of MyoFBs that contribute to remodeling during PH (Chow et al., 2013; Fatima, Zhou, & Sorrentino, 2012; D. Jun et al., 2011; Tadjali, Zhou, Rehg, & Sorrentino, 2006). These studies indicate that cells of a

stromal origin likely contribute to PF through differentiation to MyoFBs. The therapeutic effects of bone marrow-derived mesenchymal stem cells (BM-MSC) on multiple types of murine lung injury, as well as ABCG2^{pos} lung MSC on bleomycin fibrosis, further suggests that mesenchymal populations during lung injury may be reparative or pathologic depending on cellular origin or state of the microenvironment (Aslam et al., 2009; Baber et al., 2007; Gupta et al., 2007; Du Jun et al., 2011; Lee, Gupta, Serikov, & Matthay, 2009; Rojas et al., 2005; van Haaften et al., 2009).

Our previous studies established that the ABCG2 expressing resident lung mesenchymal stem cell population decreased during bleomycin fibrosis (D. Jun et al., 2011), PAH (Chow et al., 2013), and in patients with interstitial lung disease (Marriott et al., 2014) using murine models and explanted patient lung tissue (Irwin, 2007; Martin et al., 2008). Lineage tracing analysis of MSC in a hypobaric hypoxia induced murine model of PH as well as a bleomycin model of fibrosis demonstrated that these cells differentiate from non-contractile MSC to contractile MyoFB, subsequently contributing to the increased muscularization of microvessels and parenchymal remodeling characteristic of these models (Chow et al., 2013; Du Jun et al., 2011). The molecular determinants that govern ABCG2 MSC differentiation to MyoFB are unknown and represent a gap in knowledge.

The Wnt signaling pathway was previously associated with ABCG2^{pos} lung MSC transition to a MyoFB and vascular dysfunction (S. Marriott et al., 2014). Previous work has shown that the Wnt signaling pathway, in some cases downstream of TGFβ, contributes to the development of both PF and PH and represents a possible molecular basis for these diseases (Fantozzi et al., 2005; Laumanns et al., 2009; Rajkumar et al.,

2010; West et al., 2014). Wnt signaling is necessary for lung development and has been implicated in lung fibrosis, pulmonary hypertension (PH), and the formation of “plexiform lesions” in the microvasculature of both rodent models and human tissue (Akhmetshina et al., 2012; Alapati et al., 2013). Several studies have also illustrated that Wnt signaling is required for TGFβ-mediated fibrosis and the formation of MyoFB (Akhmetshina et al., 2012; Alapati et al., 2013). Both MSC and endothelial cells from PH patients demonstrated up-regulation in genes not only related to the TGFβ superfamily, but also the Wnt signaling pathway (West et al., 2014). In addition, dysfunctional TGFβ signaling underlies the pathology of PH, PF and other adult lung diseases (Fernandez & Eickelberg, 2012; Newman, Phillips, & Loyd, 2008; Yang et al., 2012). TGFβ is also associated with vascular hyperplasia and MyoFB formation during PH and bleomycin-induced fibrosis (Polosukhin et al., 2012). However, the Wnt dependent mechanism underlying the genesis of MyoFB from MSC and their participation in microvascular and parenchymal remodeling has not been defined.

Based on these data, we hypothesized that interaction between TGFβ and Wnt signaling pathways contribute to adult lung MSC differentiation. To analyze the spatiotemporal dynamics of Wnt activation in response to injury, we used fluorescence-activated cell sorting (FACS) and histological analysis of transgenic Wnt reporter mice injured with bleomycin. To test if TGFβ could induce Wnt signaling in ABCG2^{pos} MSC, we analyzed changes in gene, protein, and transcriptional expression of TGFβ induction in cultured ABCG2^{pos} MSC. We found that Wnt signaling activation occurs in ABCG2^{pos} MSC after injury, TGFβ1 treated MSC differentiate to MyoFBs, and that pyrvinium can limit this differentiation. Thus, examining the Wnt dependent mechanisms that regulate

the function of distal lung MSC may enhance the identification of clinical targets in myofibroblast driven remodeling underlying diseases such as PH, PF and ILD.

Methods

Mouse Models

All protocols were approved by the Institutional Animal Care and Use Committee at Vanderbilt University. Mice were on a C57Bl6 background. *TCF/Lef:H2B-GFP* (TOPGFP) (Ferrer-Vaquer et al., 2010; S. Marriott et al., 2014) Wnt signaling reporter mice were obtained through Jackson Laboratory (JAX stock: 013752). To identify cells that became Wnt activated during injury, mice were injured with bleomycin as described previously (D. Jun et al., 2011; S. Marriott et al., 2014). Briefly, a single intratracheal administration of bleomycin (.15U) or PBS was performed. Mice were randomized and distributed as 3-5 mice per cage for the study. Mice were euthanized during the inflammatory phase (day 2-3) or the early fibrosis phase (day 7) after injury (vehicle, n=3; inflammatory, n=4, early fibrosis, n=4). Total $GFP^{pos}/ABCG^{pos}$ cells were calculated for each mouse individually then averaged together. Female mouse were used in all bleomycin experiments.

Fluorescence-Activated Cell Sorting Analysis

Cell sorting was used to isolate $ABCG2^{pos}$ murine lung MSC from ABCG2-CreERT2 mice and quantify $eGFP^{pos}/ABCG2^{pos}$ MSCs from TOPGFP mice. To isolate cells, animals were euthanized, their lungs were removed, and mechanically homogenized. The tissue was then digested with Type 2 collagenase (Worthington, Lakewood, NJ) for 45 minutes at 37^{o}C and filtered through a 100 μm pore filter. The sample was then centrifuged for 10 minutes at 1500 RPM, the supernatant was poured off, and the cell pellet was resuspended in PBS. Cells were sorted or analyzed using a Moflo XDP cell sorter with

Summit 5.3 software (Beckman Coulter, Miami, FL). Sort mode was set to Purify 1. The cells were stained with antibodies to detect and sort $CD45^{neg}$ $ABCG2^{pos}$ cells from ABCG2-CreERT2 animals as well as GFP^{pos} $ABCG2^{pos}$ cells from TOPGFP animals. Fluorescent minus one (FMO) controls were used to set the ABCG2-PE gates. DAPI was used to exclude dead cells. The compensation controls were established as cells only, cells + DAPI + TER119, cells + APC-CD45 antibody, and cells + PE-ABCG2 antibody; alternatively, comp beads were used. The gating strategy routinely included FSC/SSC, single cells gated by SSC-W/SSC-H, FSC-W/FSC-H, and DAPI + Ter119 to gate out dead and red blood cells followed by gating on the CD45-negative population. The sort sample consisted of cells + DAPI + APC-CD45 antibody + PE-ABCG2 antibody. Again, DAPI was used to exclude dead cells. $ABCG2^{pos}$ MSC were expanded and analyzed at passage 7 (Chow et al., 2013; S. Marriott et al., 2014). Following expansion cells were analyzed by flow cytometry to confirm the presence of CD105, CD106, CD73, ScaI, and CD44 using a BD Fortessa or LSRII (BD Biosciences). The absence of c-kit, CD14, and CD45 was also confirmed.

Real-Time Quantitative PCR Analysis

To determine cellular response to TGFβ1 (10ng/mL), $ABCG2^{pos}$ MSCs were analyzed according to previous protocols (S. Marriott et al., 2014). Briefly, $ABCG2^{pos}$ MSCs were plated at a concentration of $5x10^4$ cells per well in medium containing 20% serum and incubated for 24 hours. After 24 hours, the media was changed to starvation medium containing 5% serum and incubated for 24 hours. After 24 hours in starvation medium, the untreated lysates were collected for RNA isolation (0 hour post-treatment). Treatment conditions included untreated, TGFβ1 (10ng/mL, RD Systems), DMSO control, rmWnt3a

(300 ng/mL, RD Systems), pyrvinium (200-300nM, Sigma), or bleomycin (50 μg/mL, Hospira). Lysate was harvested at 6, 24, and 48 hours post-treatment. Cell lysates were collected using lysis buffer (Qiagen, Valencia, CA) for total RNA isolation and analysis of gene expression. Quantitative PCR analysis was normalized to HPRT expression. Primers used are described in the following table. The qPCR experiments were repeated three independent times on three separate days.

Primer list

Gene Name	Forward primer	Reverse Primer
Snail	CACACGCTGCCTTGTGTCT	GGTCAGCAAAAGCACGGTT
Wisp1	CCGTGGAGCAACGGTATGAG	ACCGGGCATTGACGTTAGAG
Col1a1	GCTCCTCTTAGGGGCCACT	CCACGTCTCACCATTGGGG
Col3a1	CAAGGCTGCAAGATGGATGC	TGTCCACCAGTGCTTACGTG
MMP2	CAAGTTCCCCGGCGATGTC	TTCTGGTCAAGGTCACCTGTC
TIMP1	TGCAACTCGGACCTGGTCATA	CGCTGGTATAAGGTGGTCTCG
Axin2	TGAGATCCACGGAAACAGC	GCTGGTGCAAAGACATAGCC
SMA	GGCTTCGCTGTCTACCTTCC	AGTTGTGTGCTAGAGGCAGAG

Immunoprecipitation and Western Blotting

For protein expression analysis, cultured ABCG2 MSC (passage #30) were harvested using trypsin-EDTA (0.25%, Gibco) and pelleted through centrifugation (5 min at 1500 rpm). Media was then removed and the pellet was treated with Cytoplasmic Extraction Reagent (NE-PER Nuclear and Cytoplasmic Extraction Reagents, Thermo Scientific). Samples were incubated on ice for 10 minutes and then centrifuged at 15,000 rpm for 5 min. The cytoplasmic extract was then removed and Nuclear Extraction Reagent (NE-PER Nuclear and Cytoplasmic Extraction Reagents, Thermo Scientific) was added. Samples were incubated on ice for 40 minutes and then centrifuged at 15,000 rpm for 10 min. The nuclear extract fraction was then removed. Cytoplasmic and nuclear extract

protein concentration was determined using the Bradford assay and analyzed using a GloMax Multi-Detection System (Promega).

Protein samples were heated to 70^{o}C for 10 minutes then loaded into 10 well NuPage 4-12% Bis-Tris Gel (Novex). Samples underwent electrophoresis for 2 hours at 4^{0}C at 200V. Samples were then transferred to a nitrocellulose membrane using a tank transfer apparatus (2 hour at 4^{0}C at 200V). Nitrocellulose membranes were then blocked for 1 hour at room temperature with 5% non-fat milk in TBST. Membranes were then incubated with primary antibody for 24 hours at 4^{0}C. Primary antibodies used were total β-catenin (Cell Signaling, Cat #: 8480, 1:1500) and lamin B1 (Cell Signaling, Cat #: 12586, 1:400). After primary incubation, membranes were washed with TBST then incubated with peroxidase-conjugated AffiniPure donkey α-rabbit IgG (Jackson Immuno Research) in 5% non-fat milk in TBST for 2 hours at room temperature. Chemiluminescence was achieved by treating membranes with SuperSignal West Pico Chemiluminescent Substrate (Thermo Scientific). Western blotting experiments for TGFβ1 induced nuclear-associated β-catenin were repeated three independent times on three separate days.

Immunohistochemistry

Histological analysis was carried out by inflating murine lungs with a 1:1 solution of Optimal Cutting Temperature compound (OCT):30% sucrose and then embedding lung tissue in OCT. Tissue was then sectioned into 8 μm sections using a cryotome (Shandon). Sections were fixed in 4% PFA for 20 minutes, washed, then incubated with primary antibody in PBST+10% FBS for 24 hours at 4^{0}C. Primary antibodies include ABCG2 (CD338, Cat #: 552823, clone 5D3, BD, mouse). Sections were then incubated with

secondary antibody in PBST+10% FBS for 3 hours at room temperature. Secondary antibodies include α-mouse IgG a594 (Invitrogen, Cat #: A-11005).

Luciferase analysis

ABCG2^{pos} MSCs were plated onto 12-well plates at 3x10^4 cells per well. After 24 hours, ABCG2^{pos} MSCs were cotransfected with TOPflash and *Renilla* transfection control plasmids according to lipofectamine 2000 protocol (Life Technologies). Cells were incubated for 5 hours before transfection media was replaced with media containing 25mM LiCL or 25mM LiCL plus TGFβ1 (10ng/mL). After 24 or 48 hours, media was aspirated, lysis buffer added, and then firefly and *Renilla* luciferase activity was measured according to Dual-Luciferase Reporter Assay System protocol (Promega) using a GloMax-Multi Detection System (Promega). TGFβ1 (10ng/mL) was added 24 hours post transfection. TOPflash experiments were normalized to cotransfected *Renilla* gene expression. Luciferase experiments were repeated three independent times on three separate days.

MSC/MVEC 3D coculture

175 μl of Matrigel was added to each well of a 48 well plate and allowed to polymerize for 45 min at 37^{o}C. Lung microvasculature endothelial cells (MVEC, 1x10^6) were mixed with untreated 1x10^6 ABCG2^{pos} MSC, ABCG2^{pos} MSC treated (10 ng/mL TGFβ1) for 24 hrs, or ABCG2^{pos} MSC co-treated (10 ng/mL TGFβ1 and pyrvinium (PP, 300nM)) for 24 hrs. Cells were allowed to adhere. 75 μl of Matrigel was placed on top of cells and allowed to solidify for 45 min at 37^{o}C. 500 μl of ABCG2^{pos} MSC media was placed on top of Matrigel culture. Endothelial cord width was measured 6 hours after plating using FIJI software. Final cord widths are averages of all cord widths present in 10 individual fields.

Statistical Analysis

Mean % Wnt eGFP/ABCG2 data analyzed by one-way ANOVA followed by Tukey HSD post-hoc analysis using JMP version 5.0.12. *in vitro* data analyzed by Student's T-Test using Excel:Mac^{2011}. Significance was defined as p-value <0.05*, p-value <0.01** or p-value <0.001***.

Results

Wnt activation peaks in ABCG2^{pos} lung MSC in distal lung during the inflammatory phase following bleomycin induced fibrosis.

Since our previous studies showed that ABCG2^{pos} MSC is closely associated with adult lung microvasculature and Wnt gene expression is increased in primary endothelial cells from PH patients, we next asked if ABCG2^{pos} MSC become Wnt-activated after injury (Chow et al., 2013; D. Jun et al., 2011).

To test the spatio-temporal activation of Wnt signaling in adult lung MSC *in vivo*, *TOPGFP* mice (Fig. 2A) were intratracheally treated with bleomycin [0.15U] (Ferrer-Vaquer et al., 2010). Histological evaluation of uninjured (control) murine lung tissue sections revealed positive basal levels of nuclear GFP expression in bronchial and large airway epithelium as well as smooth muscle, indicating active Wnt signaling. During the inflammatory and early fibrosis phases following intratracheal bleomycin administration (Fig. 2A), GFP labeled nuclei were observed in the alveolar - capillary network of the adult distal lung (Fig. 2B).

We found ABCG2^{pos} /GFP^{pos} cells in distal lung during the inflammatory phase following bleomycin treatment (Fig. 1B). These data suggest that in the absence of injury, lung MSC do not exhibit detectable Wnt signaling activity. However, once an

injury occurs, Wnt signaling occurs throughout the lung, including ABCG2^{pos} MSC in the distal lung.

To quantify the change in the total number of ABCG2^{pos}/GFP^{pos} cells in the lung after injury, we used flow cytometry on cells isolated from whole adult mouse lung after injury. Overall GFP^{pos} cells in *TOPGFP* mice significantly increased (from 10.8% to 20.1%) during the inflammatory phase after injury (Fig. 2C-D). ABCG2^{pos}/GFP^{pos} cells significantly increased during the inflammatory phase as well (from 0.011% to 0.080%, Fig. 2C-D). We detected no increase in overall GFP^{pos} nor ABCG2^{pos}/GFP^{pos} cells during the early fibrotic phase (Fig. 2C-D). Thus, total Wnt-activated cells along with Wnt-activated ABCG2^{pos} MSC peak during the inflammatory phase after bleomycin injury. Importantly, CD45^{pos} cells were not included in this analysis and the Wnt activation response of immune cells was not measured.

TGFβ treatment induces transcription of Wnt target genes and myofibroblast genes in cultured ABCG2^{pos} MSC. Because ABCG2^{pos} MSC undergo active Wnt signaling after injury, and their progeny express SMA in areas of interstitial remodeling, we tested whether treating cultured ABCG2^{pos} MSCs with Wnt protein would increase MyoFB-associated gene expression.

Unexpectedly, we observed no increase in gene expression of MyoFB-associated genes (*Col1α1, MMP2, SMA, Snail, TIMP1)* after Wnt3a treatment (Fig. 3). At 24 and 48 hours posts-treatment, we observed decreases in gene expression of *Col1α1, MMP2, NG2, SMA,* and *Snail*. We observed increases in *Axin2* at 6 and 24 hours, indicating that Wnt3a treatment induces Wnt activation in these cells. Another factor that could potentially induce MSC differentiation to a MyoFB-like phenotype is

bleomycin. However, we detected no increase in MyoFB-associated gene expression after bleomycin treatment. Instead, we detected decreases in the expression of *Col1α1, MMP2, SMA, Snail, and TIMP1* (Fig. 3). Because TGFβ1 is a major contributor to the fibrotic response and is secreted by epithelial and inflammatory cells after bleomycin injury, we tested whether it could induce MyoFB differentiation (Fernandez & Eickelberg, 2012; Leask & Abraham, 2004). We found that TGFβ1 treatment increased MyoFB-associated genes (*Col1α1, MMP2, Snail, TIMP1)* at 6, 24, and 48 hours post-treatment (Fig. 3). TGFβ1 treatment also increases gene expression of *NG2,* which is found in the mature pericytes. Interestingly, we found that TGFβ1 treatment also increased expression of *Wisp1* and *Axin2*, which are known gene targets of Wnt signaling (Jho et al., 2002; Lustig et al., 2002; Shtutman et al., 1999; Tetsu & McCormick, 1999; Xu, Corcoran, Welsh, Pennica, & Levine, 2000; Yan et al., 2001). These results suggest that TGFβ1 can induce the expression of Wnt target genes. Furthermore, in contrast to Wnt3a and bleomycin treatment, addition of the pro-fibrotic stimulus TGFβ1 can induce expression of genes associated with MyoFB differentiation.

TGFβ induces Wnt activation in cultured ABCG2^{pos} MSC. Because we detected increases of *Axin2* and *Wisp1* after TGFβ1 treatment, and TGFβ1 has been shown to activate Wnt signaling in other systems (Akhmetshina et al., 2012), we next tested if TGFβ1 treatment increased nuclear β-catenin, an indicator of Wnt pathway activation (Saito-Diaz et al., 2013). TGFβ1 treatment increased not only the level of cytoplasmic β-catenin also nuclear β-catenin (Fig. 4A). These immunolocalization studies were confirmed biochemically by immunoblotting for β-catenin in the nuclear fraction (Fig.

4B). Finally, we show that TGFβ1 induced ABCG2^{pos} MSC also acquire SMA stress fibers (Fig. 4C).

If TGFβ1 activates Wnt signaling during the MSC-MyoFB transition, it is possible that decreasing Wnt activity could block this differentiation event. To test this possibility, we co-treated cultured ABCG2^{pos} MSCs with TGFβ1 and the small molecule Wnt inhibitor pyrvinium, which promotes the degradation of the Wnt pathway components β-catenin and Pygopus 2 (Thorne et al., 2010). We found that pyrvinium inhibited TGFβ1 induced Wnt activation (as indicated by increased luciferase activity from a transfected Wnt reporter plasmid) in ABCG2^{pos} MSCs (Fig. 5A). Pyrvinium co-treatment also inhibited TGFβ1 induced *Axin2* gene expression as well as several MyoFB genes in cultured ABCG2^{pos} MSCs (Fig. 5B). Thus, pyrvinium decreases TGFβ1 induced Wnt gene expression and MyoFB gene expression.

Because pericytes closely adhere to microvascular endothelial cells and facilitate angiogenesis (Bergers & Song 2005), I next tested if TGFβ1 treatment of ABCG2^{pos} MSCs co-cultured with microvascular lung endothelial cells (luMVEC) prevents angiogenesis. MVECs form cord-like structures reminiscent of blood vessels when cultured in Matrigel and co-culturing MVECs with pericytes can alter the formation of these structures (Stratman et al., 2009). I observed an increase in the width of cord-like structures formed by ABCG2^{pos} MSCs co-cultured with luMVEC upon pre-treatment with TGFβ1 (Fig. 6 A-B). Pyrvinium blocked the TGFβ1-mediated width increase of these cord-like structures. These results indicate that TGFβ1 treatment induces increased width in the cord structures formed by ABCG2^{pos} MSCs cultured with lung MVEC and that pyrvinium can reverse these changes.

Discussion

In the current studies, I provide evidence that adult lung MSC respond to bleomycin injury by increasing expression of Wnt signaling during the inflammatory phase and that this increase in expression is associated with MSC-to-MyoFB differentiation. Using FACs and histological analyses of *TOPGFP* animals I show that Wnt activation in lung MSC increase during the inflammatory phase after bleomycin injury. I demonstrated that TGFβ induced expression of MyoFB and Wnt target genes in cultured ABCG2 MSCs by quantitative qPCR and that TGFβ1 induced activation of a *TOPFLASH* reporter. I showed that pyrvinium, a small molecule that potentiates the activity of CK1α and increases β-catenin degradation, decreases TGFβ1 induction of endogenous Wnt and MyoFB target genes as well as TGFβ1 induced *TOPFLASH* expression. Finally, I found that pyrvinium was able to prevent abnormal structures induced by TGFβ1 pretreatment of ABCG2^{pos} MSC-luMVEC in co-cultures.

Based on these *in vitro* studies and previous work, I hypothesize that the observed Wnt pathway activation in ABGC2 MSC during the inflammatory phase is a combination of Wnt ligands released during injury and the action of TGFβ1 secreted by injured epithelial cells and inflammatory cells (Figure 7). Several studies showed that protein expression of β-catenin is increased in whole lung extracts of bleomycin-injured animals (Henderson et al., 2010; Wang et al., 2014). Immunohistochemistry identified nuclear β-catenin in mouse bronchial and epithelial cells post-bleomycin injury (Kim et al., 2011; Konigshoff et al., 2009). This increase in nuclear β-catenin agrees with lacZ expression of the alveolar epithelium in a bleomycin injured Wnt reporter animal model *TOPGAL* (Henderson et al., 2010; Konigshoff et al., 2009). While these studies show

Wnt activation in alveolar epithelium as well as resident MSC in injured animals, the major cell type that is responsible for production of Wnt ligands during injury remains unclear. However, several injury and developmental studies indicate that Wnt ligands may be secreted from epithelial cells and fibroblasts. Immunohistochemistry of bleomycin injured mice lungs showed Wnt-1 and Wnt-10b expression in lung fibroblasts as well as several unidentified cell-types (Akhmetshina et al., 2012). *In situ* hybridization showed that during mouse lung development, airway epithelium secrete Wnt7b and airway mesenchyme secrete Wnt2 (Weidenfeld, Shu, Zhang, Millar, & Morrisey, 2002). Interestingly, during human lung morphogenesis the airway epithelium express Wnt7b and Wnt2 (Zhang, Shi, Huang, & Lai, 2012). These studies indicate that developmentally, the epithelium can secrete Wnt ligands, a capability that may be recapitulated during injury. Another source of Wnt activation may be TGFβ secreted by epithelial and immune cells during injury. Consistent with our data, TGFβ induction has been shown to increase gene expression of Wnt5B and β-catenin in human lung MRC-5 fibroblasts (Baarsma et al., 2011). TGFβ induction has also been previously shown to induce nuclear β-catenin and activate *TOPFLASH* reporter activity in human dermal fibroblasts (Akhmetshina et al., 2012).

Our observation that the Wnt inhibitor, pyrvinium, decreases expression of TGFβ1 induced MyoFB genes may indicate that Wnt signaling plays a role in MyoFB differentiation. Treatment of BM-MSC derived from Sprague-Dawley rats with recombinant Wnt3a results in increased levels of β-catenin as well as an increased expression of αSMA protein (Sun et al., 2014). Recombinant Wnt1 has also been shown to increase the activity of a *Col1α2* promoter and the amount of SMA in human

dermal fibroblasts. Transgenic animals that overexpress the Wnt inhibitor, DKK1, have decreased a MyoFB population after bleomycin injury (Akhmetshina et al., 2012). DKK1 and pyrvinium have been shown to exhibit anti-fibrogenic effects in other organs, such as the kidney and the heart. Kidney pericytes and myofibroblasts derived from mice with unilateral uretic obstruction (UUO) injury had increased MyoFB and Wnt target gene expression, and cultured kidney pericytes treated with TGFβ1 increase *αSMA*, *CTGF*, and *Col1α1* gene expression. Adenoviral delivery of DKK1 mRNA decreased Col1α1^{pos} and αSMA ^{pos} cells post-UUO injury (Ren et al., 2013). Oral administration of pyrvinium after experimental myocardial infarction decreases fibrotic area and αSMA^{pos} myofibroblasts in infarcted hearts, and direct injection of pyrvinium into cardiac tissue of infarcted hearts decreases adverse cardiac remodeling as measured by left ventricular internal diameter in diastole (LVIDD) (Murakoshi, Saiki, Urayama, & Sato, 2013; Saraswati et al., 2010).

Multiple groups have investigated the mechanism by which TGFβ induces Wnt signaling. Akhmetshina and colleagues provide evidence that TGFβ1 treatment in dermal fibroblasts decreases DKK1 mRNA and protein expression (Akhmetshina et al., 2012). Many genes related to development are co-regulated by TGFβ and Wnt signaling at the level of transcription (Guo & Wang, 2009). However, I was unable to identify known Wnt responsive elements in key MyoFB genes such as *αSMA*. It is possible that the interaction between Wnt and TGFβ is context dependent. Thus, DKK1 downregulation in dermal fibroblasts represents one of many possible mechanisms by which TGFβ can activate the Wnt pathway.

There are several limitations to our current studies. Although bleomycin injured animals develop interstitial remodeling, they do not develop fibroblast foci, a common feature observed in human PF. Thus, bleomycin injury can recapitulate only some components of human lung fibrotic disorders. In addition, TGFβ1 represents only one of many profibrotic factors in the disease microenvironment. Other chemokines and cytokines likely interact with Wnt and TGFβ signaling to influence the MSC phenotype. Another major limitation is the potential off-target effects of pyrvinium. Pyrvinium acts as a CK1α agonists. Because CK1α interacts with a several different pathways, this raises the possibility that the effect of pyrvinium is not due to its action in the Wnt pathway. Future directions would include identifying cells that secrete Wnt ligands in the alveolar unit, testing for cooperative effects of Wnt signaling and TGFβ signaling on MSC-MyoFB transition, and evaluating the mechanism governing the connection between Wnt/β-catenin and TGFβ in ABCG2^{pos} MSC.

My current research provides a foundation for future clinical studies that focus on altering resident organ MSC populations through pharmacological means. Clinical trials are ongoing to test the applicability of small molecule inhibitors to Wnt and TGFβ signaling for the treatment of a variety of fibrotic disorders. My studies suggest that co-treatment with inhibitors of the Wnt and TGFβ signaling pathways at specific times post-injury may improve remodeling via a mechanism involving retention of a resident stem cell population. *This work was performed in the lab of Dr. Susan Majka. Christa Gaskill and Shennea Marriott contributed to this work.

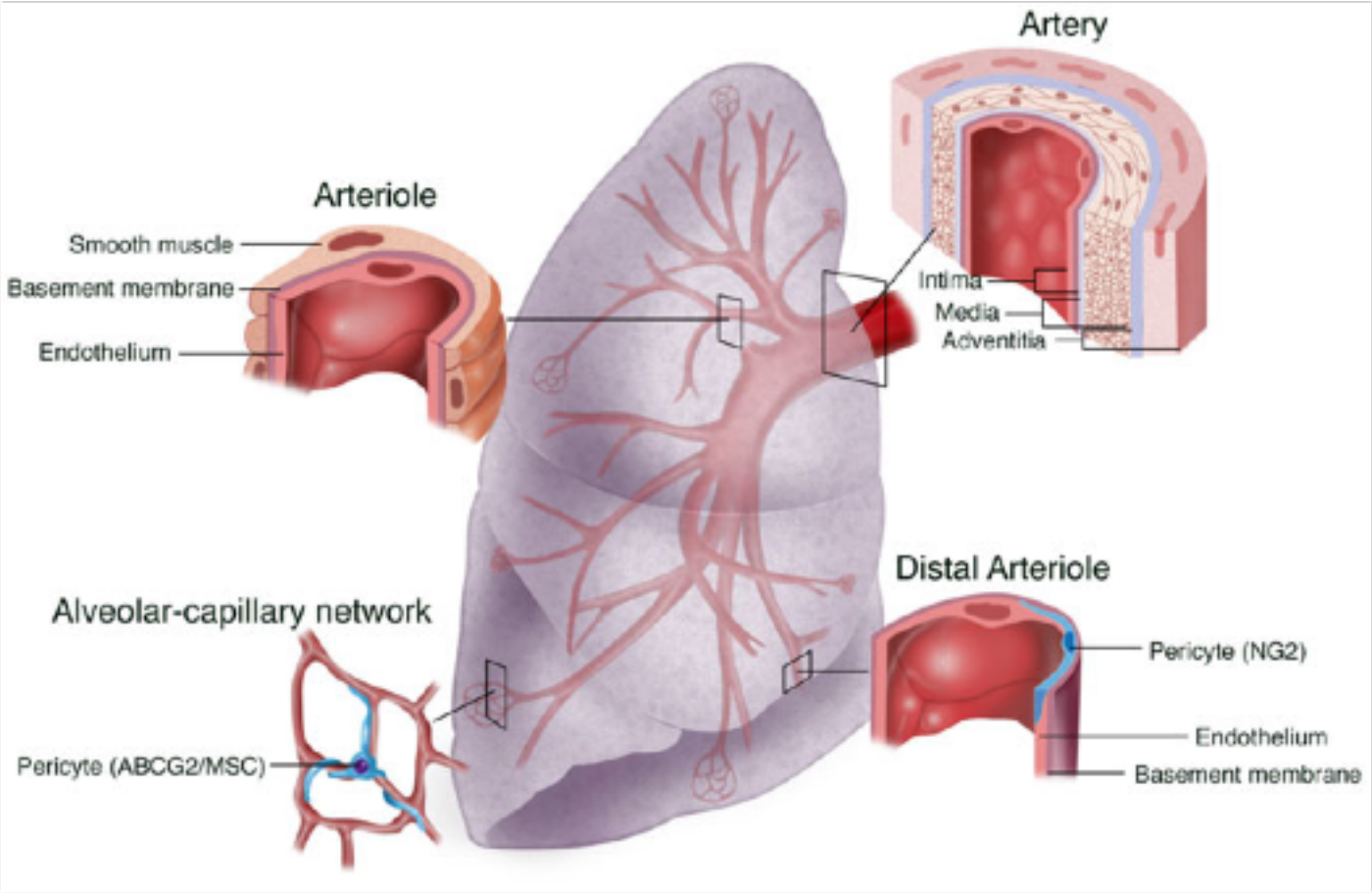

Figure 1 The pulmonary arterial vascular tree. The pulmonary arterial circulation is characterized by a gradual loss of complexity and muscularization from proximal to distal branches of the vascular tree (Townsley 2012). The pulmonary artery is the most proximal and muscularized portion of the arterial circulation. The pulmonary artery consists of defined layers, including the intima (endothelium), the media (smooth muscle), and the adventitia (fibroblasts, microvessels, and vascular precursors). The branching smaller arteries, also referred to as arterioles, are defined by size and muscularization. The small artery/arteriole is composed of 1–2 layers of smooth muscle which completely encircle the endothelium of the vessels. With further branching, smooth muscle becomes less continuous and the most distal vessels and capillaries, consisting of endothelial cells forming a small diameter conduit, are stabilized by a non-continuous layer of pericytes. Pericytes are directly in contact with the endothelium and reside under a continuous basement membrane.

Results

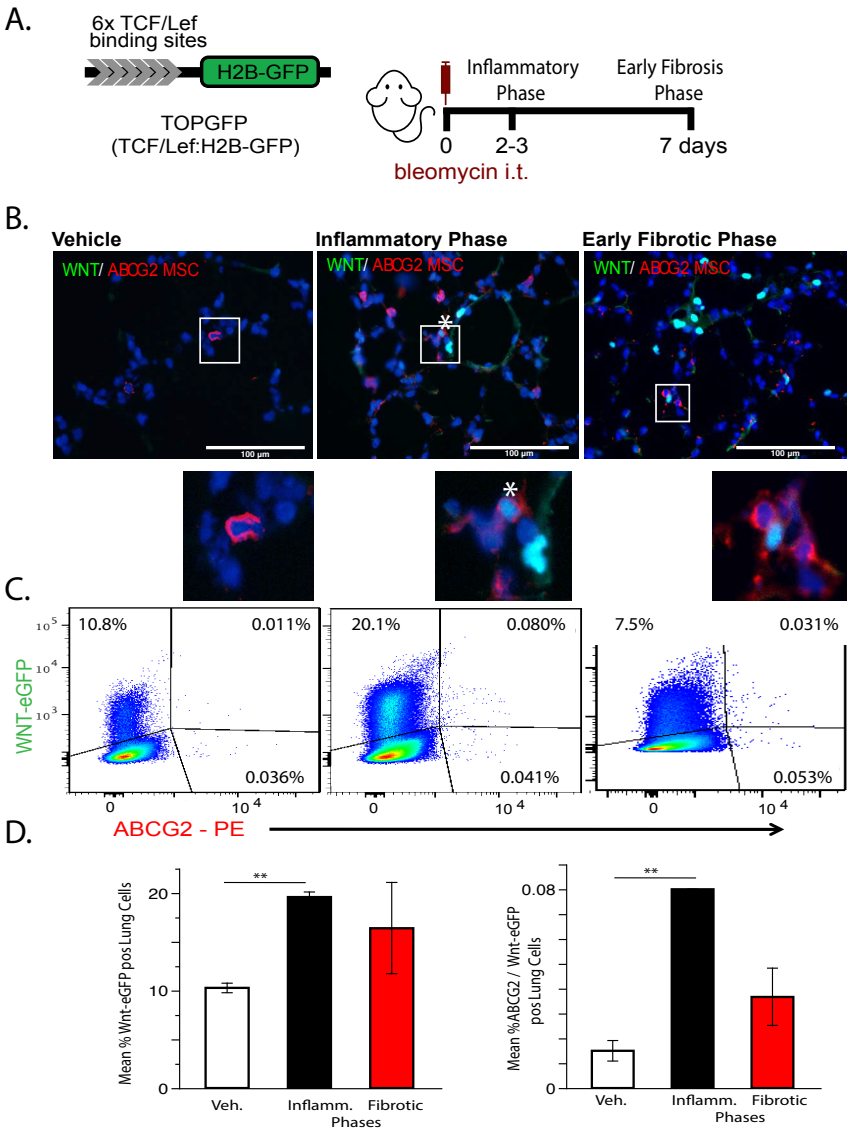

Figure 2 Wnt signaling in ABCG2^{pos} lung MSC peaks during the inflammatory phase of bleomycin Injury and fibrosis. **(A)** The left panel provides a description of the TOPGFP Wnt reporter animal. The right panel details the bleomycin injury model. Animals were administered a single dose of bleomycin (.15 U) intratracheally and analyzed during the inflammatory (days 2-3) and early fibrosis (day 7) phase after injury. **(B)** Epifluorescence imaging of colabeling between cells with active Wnt signaling and ABCG2 expression in the distal lung during the inflammatory and early fibrotic phases after injury. Cells with active Wnt signaling shown with nuclei in green. ABCG2^{pos} cells shown in red. Scale bar represents 100 μm. **(C)** Representative FACS staining profiles of GFP^{pos} (vertical axis)/ABCG2^{pos} cells (horizontal axis) single cell suspensions of whole murine lung digested by collagenase from TOPGFP animals during the inflammatory (days 2-3) and early fibrosis (day 7) phase after injury. **(D)** The quantification of total GFP^{pos} cells in (A-C) is shown on the left panel. The quantification of total GFP^{pos}/ABCG2^{pos} cells in (A-C) is shown on the right panel. Data presented in text as (SE). Vehicle n=3. Inflammatory Phase n=4. Early Fibrotic Phase n=4.

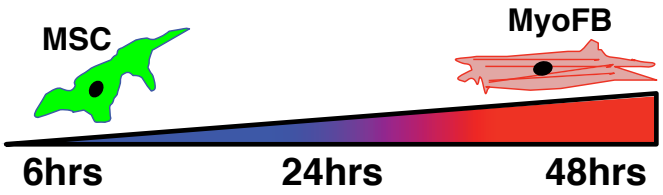

A. Wnt3a (200 ng/mL)

6hrs	24hrs	48hrs
Axin2**	**Axin2****	NG2*
Wisp1*	Col1α1*	SMA**
	MMP2**	Snail**
	NG2*	**WISP1***
	Snail*	
	WISP1*	

B. Bleomycin (50 μg/mL)

6hrs	24hrs	48hrs
Col1α1*	Col1α1*	Col1α1*
MMP2*	MMP2*	**WISP1***
SMA*	SMA**	
TIMP1*	Snail*	
	WISP1*	

C. TGFβ (10 ng/mL)

6hrs	24hrs	48hrs
MMP2**	**Axin2****	Col1α*
NG2**	Col1α1*	TIMP1**
Snail**	MMP2**	**WISP1***
TIMP1*	NG2*	
WISP1**	SMA*	
	Snail**	
	TIMP1**	
	WISP1*	

Figure 3 TGFβ1 treatment induces MyoFB gene expression in cultured ABCG2^{pos} MSC. Diagram in upper panel provides a description of MSC-MyoFB transition. **(A-C)** Gene expression changes in cultured ABCG2^{pos} MSC (passage #25) after 6, 24, or 48 hr treatment with bleomycin (50ug/mL), recombinant Wnt3a (200 ng/mL), or recombinant TGFβ1 (10 ng/mL). RNA was collected and amplified by qPCR. Two individual cell samples were run in triplicate during qPCR analyses. Fold change relative to control was calculated using delta delta-CT method. 3 independent replicates performed using ABCG2^{pos} MSC line--representative experiment shown. Genes that were significantly increased after treatment are shown in red. Genes that were significantly decreased after treatment are shown in blue. Wnt target genes are bolded. Asterisks correspond to significance. * p<.05. ** p<.01. *** p<.001.

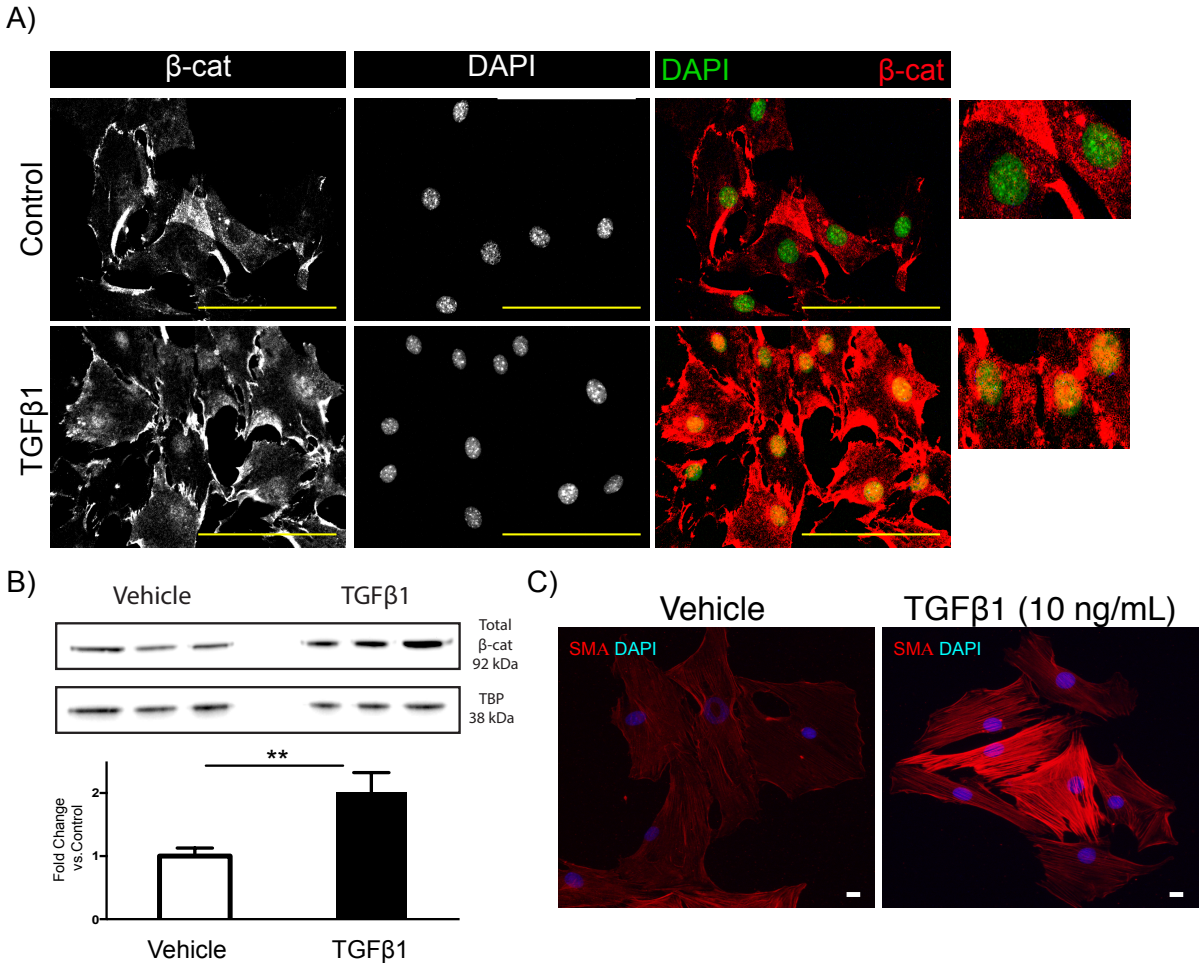

Figure 4 TGFβ1 induces Wnt activation in cultured ABCG2^{pos}. **(A)** Immunofluorescent staining on TGFβ1-treated (10ng/mL) ABCG2^{pos} MSC. DAPI shown in green. β-cat shown in red. Scale bar = 100μm. **(B)** Western blotting for total β-cat in the nuclear fraction of TGFβ1-treated (10ng/mL, 30min) cultured MSCs. Two independent replicates performed using ABCG2^{pos} MSC line. *Lower panel* Quantification of total nuclear associated β-cat from biological replicates of TGFβ1 induced ABCG2^{pos} MSC. Data are presented as (SD). Values standardized to TBP loading controls. ** p<.01 **(C)** Immunofluorescent staining on TGFβ1-treated ABCG2^{pos} MSC. DAPI shown in blue. SMA shown in red. Scale bar = 10μm.

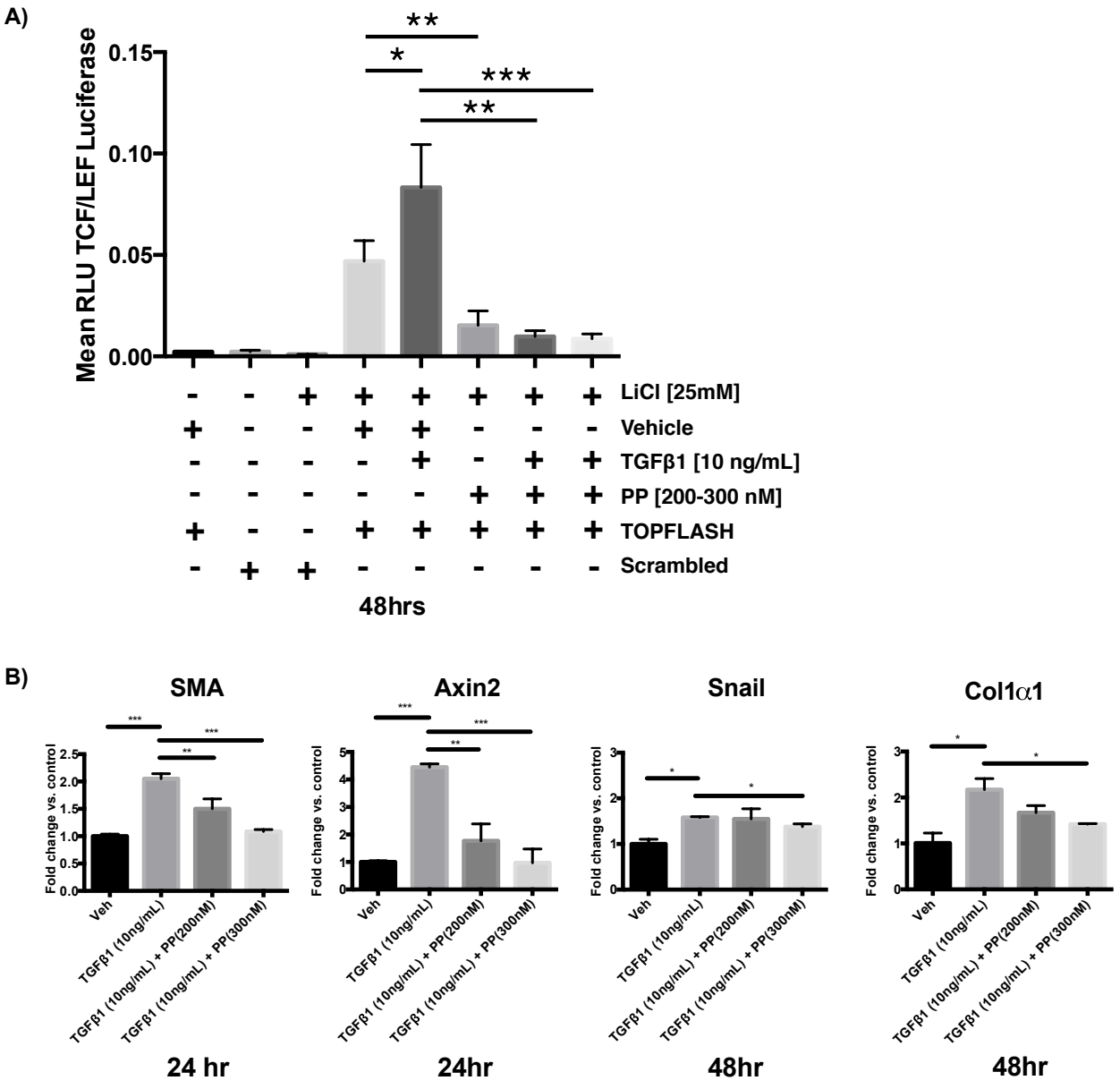

Figure 5 Pyrvinium decreases expression of MyoFB target genes. **(A)** Quantification of luciferase activity from TGFβ1 induced ABCG2^{pos} MSC transfected with a TOPflash reporter construct and *Renilla* luciferase. MSC transfected for 5hrs in OptiMEM Media, incubated for 24hrs in 20% FBS+DMEM, then treated for 48hrs with TGFβ1 or pyrvinium. Two individual cell samples were run in triplicate during luciferase analysis. Two independent replicates performed using ABCG2^{pos} MSC line-representative experiment shown. Data are presented as (SD). **(B)** TGFβ1-induced gene expression changes in cultured ABCG2^{pos} MSC co-treated with pyrvinium (200-300nM). UT = untreated. Veh= 0.01% DMSO. *SMA* = smooth muscle actin. *Col1α1* = collagen 1 alpha 1. Two independent replicates performed using ABCG2^{pos} MSC line-representative experiment shown.

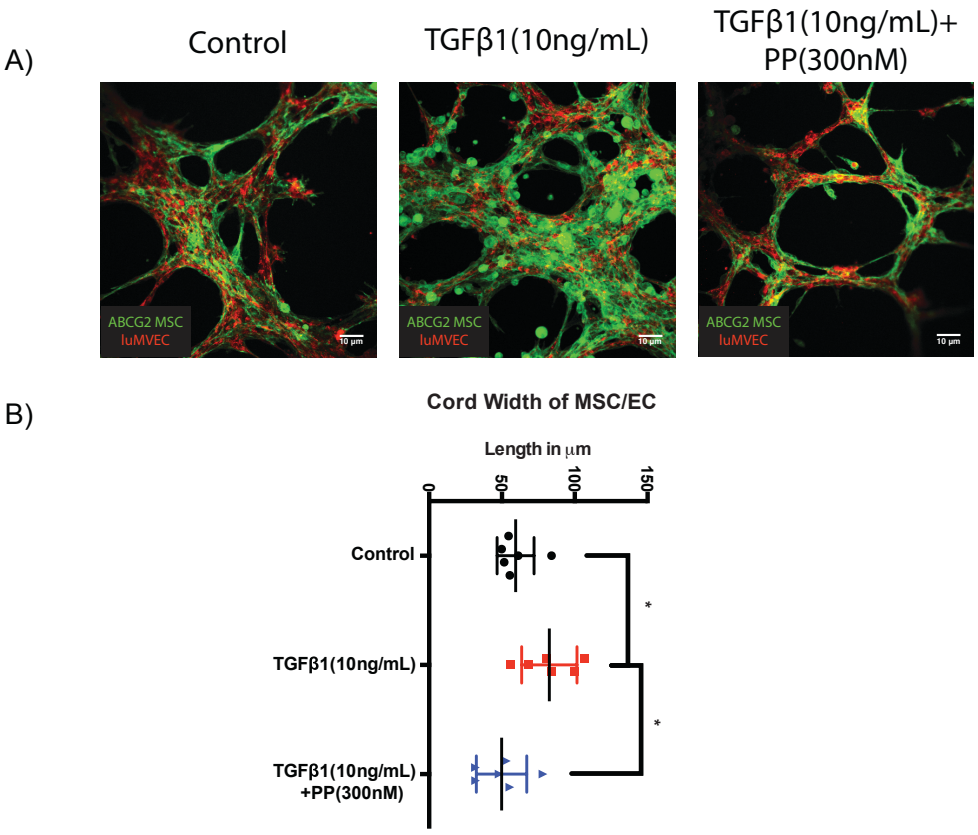

Figure 6 TGFβ1 induces cord thickening in ABCG2^{pos} MSC in 3D Matrigel co-culture with microvascular endothelial cells. **(A)** ABCG2^{pos} MSC (green) were pretreated with TGFβ1 (10ng/mL) or TGFβ1 (10ng/mL) + pyrvinium (300nM) for 24 hr prior to co-culture with microvascular endothelial cells labeled with a cellular dye (red). ABCG2^{pos} MSCs and MVEC were cultured for 6 hours prior to cord width measurement. **(B)** Quantification of cord width measurement for ABCG2^{pos} MSC/MVEC 3D Matrigel co-culture.

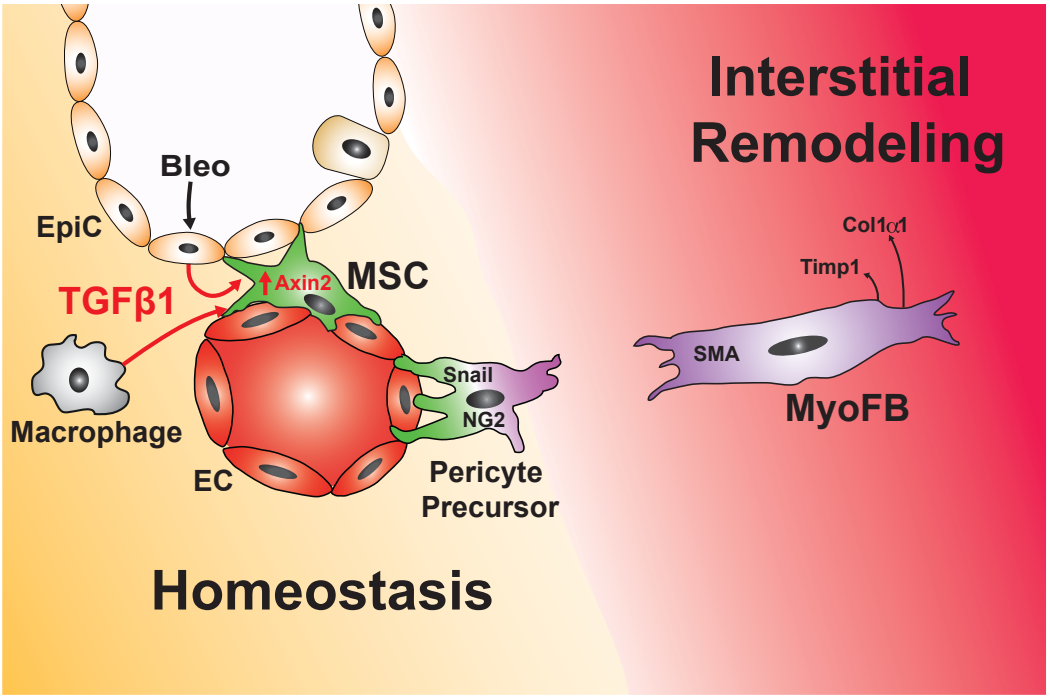

Figure 7 Model of bleomycin induced ABCG2^{pos} to MyoFB transition in the adult lung. Bleomycin injury induces TGFβ1 release from injured epithelium and neighboring cell types. TGFβ1 released by injured epithelium and neighboring cells induces the release of Wnt proteins from MSCs as well as increases intracellular beta-catenin in MSCs. These MSC begin to express Snail and NG2 and transition to a pericyte precursor. These pericyte precursors express SMA and begin to secrete Col1α1. Pyrvinium decreases the expression of several genes associated with MyoFBs as well as decreases expression of TGFβ1 induced Wnt target genes.

Future Directions

Idiopathic pulmonary fibrosis (IPF) is a disease of unknown etiology that is associated with an increase in Wnt activation and a decrease in total MSC in the lungs of IPF patients (Marriott 2014, Wang 2014). One of the key questions raised by this work is how canonical Wnt signaling regulates MSC differentiation to MyoFB and subsequent microvascular remodeling *in vivo.* An inducible ABCG2 MSC lineage tracing model system can be used to selectively activate/inhibit Wnt signaling in MSC by overexpressing/knocking out β-catenin in a bleomycin injury model. These mice would allow for conditional lineage labeling and overexpression (OE)/knock-out (KO) of β-catenin in ABCG2 MSC. In addition, the analysis of MSC fate as well as the resulting vascular and pulmonary physiology following bleomycin injury can be performed. To test for the outcomes of bleomycin injury, pulmonary leak, microvessel loss, muscularization and right ventricular systolic pressure (RVSP) can be measured on days 2-4, 7, 14 or 35 post bleomycin injury. I predict that following bleomycin injury, ABCG2 MSC will increase canonical Wnt signaling in coordination with MyoFB differentiation, which will result in increased vascular leak, microvessel loss, muscularization and a decline in vascular and pulmonary function. If this hypothesis is correct, ABCG2 β-catenin OE and ABCG2 β-catenin KO animals will have worse and better outcome, respectively, as measured by vascular leak, microvessel loss, muscularization and a decline in vascular and pulmonary function. These observations would support my hypothesis that

canonical Wnt activation is necessary for ABCG2-derived MyoFB differentiation and that these ABCG2-derived MyoFB are maladaptive in pulmonary hypertension.

These experiments also raise the question as to the mechanistic interaction between MSC and EC populations in the adult lung after injury. Given that ABCG2 MSCs are pericytes likely respond to Wnt ligands secreted by lung endothelial cells, the interaction between these two cell populations likely plays a key role in injury response. However, one of the major obstacles with examining the interplay between MSC and ECs has been the lack of an adequate *in vitro* co-culturing system that faithfully mimics their *in vivo* interaction. Based on the complex paracrine interactions that take place between ECs and mesenchymal cells, an *in vitro* system that recapitulates the unique microenvironment of the lung parenchyma is needed. Such a system may involve the use of a Matrigel-based 3D co-culture system that will allow testing of the underlying mechanisms by which increased Wnt signaling in ABCG2-MSC affects nearby endothelial cells. One hypothesis is that ABCG2-derived MyoFBs regulate vasculature by altering the tubule formation patterns of EC networks as well as the ability of ABCG2 MSCs to attach to ECs following Wnt activation. To test this possibility, ABCG2 MSCs can be treated with recombinant TGFβ1 for 48 hours to increase Wnt signaling and then co-cultured with primary lung microvascular ECs in Matrigel. Assay endpoints will include tubule number, length, number of branch points, and the number of ABCG2 MSCs co-labeling with ECs. The effect of Wnt inhibitors on these readouts can also be examined. I predict that TGFβ1 treated MSCs will decrease EC branching and overall MSC/EC association as MSCs differentiate to a MyoFB-like cell.

There are two important questions that can be readily addressed in the *in vivo* model: 1) what cells are secreting TGFβ1 in the distal vasculature after bleomycin injury that affect ABCG2 MSCs and 2) what gene expression changes occur in ABCG2 MSC cells post-injury? To address the first questions, *in situ* hybridization with probes directed against TGFβ1 can be performed on mouse adult lung tissue on days 2-4, 7, 14 and 35 post-bleomycin injury, and the cell type expressing TGFβ1 nearby ABCG2 MSCs can be identified. To address the second question, a bigenic animal can be generated by crossing an ABCG2-CreERT2 driver mouse to mice expressing the Rosa26 mT/mGFP reporter. ABCG2 MSCs can be isolated via flow cytometry and analyzed through qPCR to determine if the genes upregulated in TGFβ1 treated cultured MSC are the same genes upregulated during bleomycin injury.

While I have shown that TGFβ1 increases Wnt signaling in cultured ABCG2 MSC, I have not identified the mechanism for this cross talk. To begin to understand the mechanism by which TGFβ1 acts on the Wnt pathway, other indicators of Wnt pathway activation can be evaluated and epistatic experiments performed. Cultured MSC can be treated with TGFβ1 and phospho-LRP6 expression (indicative of Wnt receptor activation) determined. This experiment will determine if the membrane components of Wnt signaling are involved in this crosstalk. In addition, ABCG2 MSCs can be treated with TGFβ1, LRP6 siRNA transfected, and Wnt target gene expression analyzed by qPCR to further test if cross talk occurs at the level of the membrane. Treatment of ABCG2 MSCs with Wnt inhibitors with mechanisms-of-action distinct from pyrvinium (such as XAV939 or IWR) can be performed to confirm that the effects of pyrvinium in

blocking TGFβ1-mediated ABCG2 MSC-to-MyoFB transition is due to its capacity to inhibit Wnt signaling.

Finally, CoIPs between β-catenin and Smad2 or Smad3 in HEK293 STF cells can be performed as they have been shown to interact and increase transcription of Wnt pathway target genes (Hirota et al., 2008). As it has also been reported that TGFβ1 activates Wnt signaling by decreasing Dkk1, Dkk1 gene expression can be analyzed via qPCR and immunoblotting in TGFβ1-treated ABCG2 MSC (Akhmetshina 2012). Research into the mechanism of cross talk between these two pathways (Wnt and TGFβ1) post-injury will allow for the development of novel therapies to treat multiple devastating diseases.

References

Akhmetshina, A., Palumbo, K., Dees, C., Bergmann, C., Venalis, P., Zerr, P., . . . Distler, J. H. (2012). Activation of canonical Wnt signalling is required for TGFbeta-mediated fibrosis. *Nat Commun, 3*, 735. doi:10.1038/ncomms1734

Alapati, D., Rong, M., Chen, S., Lin, C., Li, Y., & Wu, S. (2013). Inhibition of LRP5/6-mediated Wnt/beta-catenin signaling by Mesd attenuates hyperoxia-induced pulmonary hypertension in neonatal rats. *Pediatr Res, 73*(6), 719-725. doi:10.1038/pr.2013.42

Aslam, M., Baveja, R., Liang, O. D., Fernandez-Gonzalez, A., Lee, C., Mitsialis, S. A., & Kourembanas, S. (2009). Bone marrow stromal cells attenuate lung injury in a murine model of neonatal chronic lung disease. *Am J Respir Crit Care Med, 180*(11), 1122-1130. doi:10.1164/rccm.200902-0242OC

Baarsma, H. A., Spanjer, A. I., Haitsma, G., Engelbertink, L. H., Meurs, H., Jonker, M. R., . . . Gosens, R. (2011). Activation of WNT/beta-catenin signaling in pulmonary fibroblasts by TGFbeta(1) is increased in chronic obstructive pulmonary disease. *PLoS One, 6*(9), e25450. doi:10.1371/journal.pone.0025450

Baber, S. R., Deng, W., Master, R. G., Bunnell, B. A., Taylor, B. K., Murthy, S. N., . . . Kadowitz, P. J. (2007). Intratracheal mesenchymal stem cell administration attenuates monocrotaline-induced pulmonary hypertension and endothelial dysfunction. *Am J Physiol Heart Circ Physiol, 292*(2), H1120-1128. doi:10.1152/ajpheart.00173.2006

Chow, K., Fessel, J. P., Kaoriihida, S., Schmidt, E. P., Gaskill, C., Alvarez, D., . . . Majka, S. M. (2013). Dysfunctional resident lung mesenchymal stem cells contribute to pulmonary microvascular remodeling. *Pulm Circ, 3*(1), 31-49. doi:10.4103/2045-8932.109912

Fantozzi, I., Huang, W., Zhang, J., Zhang, S., Platoshyn, O., Remillard, C. V., . . . Yuan, J. X. (2005). Divergent effects of BMP-2 on gene expression in pulmonary artery smooth muscle cells from normal subjects and patients with idiopathic pulmonary arterial hypertension. *Exp Lung Res, 31*(8), 783-806. doi:10.1080/01902140500461026

Fatima, S., Zhou, S., & Sorrentino, B. P. (2012). Abcg2 expression marks tissue-specific stem cells in multiple organs in a mouse progeny tracking model. *Stem Cells, 30*(2), 210-221. doi:10.1002/stem.1002

Fernandez, I. E., & Eickelberg, O. (2012). The impact of TGFbeta on lung fibrosis: from targeting to biomarkers. *Proc Am Thorac Soc, 9*(3), 111-116. doi:10.1513/pats.201203-023AW

Ferrer-Vaquer, A., Piliszek, A., Tian, G., Aho, R. J., Dufort, D., & Hadjantonakis, A. K. (2010). A sensitive and bright single-cell resolution live imaging reporter of Wnt/ss-catenin signaling in the mouse. *BMC Dev Biol, 10*, 121. doi:10.1186/1471-213X-10-121

Guo, X., & Wang, X. F. (2009). Signaling cross-talk between TGFbeta/BMP and other pathways. *Cell Res, 19*(1), 71-88. doi:10.1038/cr.2008.302

Gupta, N., Su, X., Popov, B., Lee, J. W., Serikov, V., & Matthay, M. A. (2007). Intrapulmonary delivery of bone marrow-derived mesenchymal stem cells

improves survival and attenuates endotoxin-induced acute lung injury in mice. *J Immunol, 179*(3), 1855-1863.
Henderson, W. R., Jr., Chi, E. Y., Ye, X., Nguyen, C., Tien, Y. T., Zhou, B., . . . Kahn, M. (2010). Inhibition of Wnt/beta-catenin/CREB binding protein (CBP) signaling reverses pulmonary fibrosis. *Proc Natl Acad Sci U S A, 107*(32), 14309-14314. doi:10.1073/pnas.1001520107
Irwin, D., Helm K, Campbell N, Imamura M, Fagan K, Harral J, Carr M, Young KA, Klemm D, Gebb S, Dempsey EC, West J, Majka S. (2007). Neonatal lung side population cells demonstrate endothelial potential and are altered in response to hyperoxia-induced lung simplification. *Am J Physiol Lung Cell Mol Physiol. , 293*, L941-951.
Jho, E. H., Zhang, T., Domon, C., Joo, C. K., Freund, J. N., & Costantini, F. (2002). Wnt/beta-catenin/Tcf signaling induces the transcription of Axin2, a negative regulator of the signaling pathway. *Mol Cell Biol, 22*(4), 1172-1183.
Jun, D., Garat, C., West, J., Thorn, N., Chow, K., Cleaver, T., . . . Majka, S. M. (2011). The pathology of bleomycin-induced fibrosis is associated with loss of resident lung mesenchymal stem cells that regulate effector T-cell proliferation. *Stem Cells, 29*(4), 725-735. doi:10.1002/stem.604
Jun, D., Garat, C., West, J., Thorn, N., Chow, K., Cleaver, T., . . . Majka, S. M. (2011). The Pathology of Bleomycin-Induced Fibrosis Is Associated with Loss of Resident Lung Mesenchymal Stem Cells That Regulate Effector T-cell Proliferation. *STEM CELLS, 29*(4), 725-735. doi:10.1002/stem.604
Kim, T. H., Kim, S. H., Seo, J. Y., Chung, H., Kwak, H. J., Lee, S. K., . . . Sohn, J. W. (2011). Blockade of the Wnt/beta-catenin pathway attenuates bleomycin-induced pulmonary fibrosis. *Tohoku J Exp Med, 223*(1), 45-54.
Konigshoff, M., Kramer, M., Balsara, N., Wilhelm, J., Amarie, O. V., Jahn, A., . . . Eickelberg, O. (2009). WNT1-inducible signaling protein-1 mediates pulmonary fibrosis in mice and is upregulated in humans with idiopathic pulmonary fibrosis. *J Clin Invest, 119*(4), 772-787. doi:10.1172/JCI33950
Laumanns, I. P., Fink, L., Wilhelm, J., Wolff, J. C., Mitnacht-Kraus, R., Graef-Hoechst, S., . . . Voswinckel, R. (2009). The noncanonical WNT pathway is operative in idiopathic pulmonary arterial hypertension. *Am J Respir Cell Mol Biol, 40*(6), 683-691. doi:10.1165/rcmb.2008-0153OC
Leask, A., & Abraham, D. J. (2004). TGFbeta signaling and the fibrotic response. *FASEB J, 18*(7), 816-827. doi:10.1096/fj.03-1273rev
Lee, J. W., Gupta, N., Serikov, V., & Matthay, M. A. (2009). Potential application of mesenchymal stem cells in acute lung injury. *Expert Opin Biol Ther, 9*(10), 1259-1270. doi:10.1517/14712590903213651
Lustig, B., Jerchow, B., Sachs, M., Weiler, S., Pietsch, T., Karsten, U., . . . Behrens, J. (2002). Negative feedback loop of Wnt signaling through upregulation of conductin/axin2 in colorectal and liver tumors. *Mol Cell Biol, 22*(4), 1184-1193.
Marriott, S., Baskir, R. S., Gaskill, C., Menon, S., Carrier, E. J., Williams, J., . . . Majka, S. M. (2014). ABCG2pos lung mesenchymal stem cells are a novel pericyte subpopulation that contributes to fibrotic remodeling. *Am J Physiol Cell Physiol, 307*(8), C684-698. doi:10.1152/ajpcell.00114.2014

Martin, J., Helm, K., Ruegg, P., Varella-Garcia, M., Burnham, E., & Majka, S. (2008). Adult lung side population cells have mesenchymal stem cell potential. *Cytotherapy, 10*(2), 140-151. doi:doi:10.1080/14653240801895296
McNulty, K., & Janes, S. M. (2012). Stem cells and pulmonary fibrosis: cause or cure? *Proc Am Thorac Soc, 9*(3), 164-171. doi:10.1513/pats.201201-010AW
Murakoshi, M., Saiki, K., Urayama, K., & Sato, T. N. (2013). An anthelmintic drug, pyrvinium pamoate, thwarts fibrosis and ameliorates myocardial contractile dysfunction in a mouse model of myocardial infarction. *PLoS One, 8*(11), e79374. doi:10.1371/journal.pone.0079374
Newman, J. H., Phillips, J. A., 3rd, & Loyd, J. E. (2008). Narrative review: the enigma of pulmonary arterial hypertension: new insights from genetic studies. *Ann Intern Med, 148*(4), 278-283.
Noble, P. W., Barkauskas, C. E., & Jiang, D. (2012). Pulmonary fibrosis: patterns and perpetrators. *J Clin Invest, 122*(8), 2756-2762. doi:10.1172/JCI60323
Phan, S. H. (2012). Genesis of the myofibroblast in lung injury and fibrosis. *Proc Am Thorac Soc, 9*(3), 148-152. doi:10.1513/pats.201201-011AW
Polosukhin, V. V., Degryse, A. L., Newcomb, D. C., Jones, B. R., Ware, L. B., Lee, J. W., . . . Lawson, W. E. (2012). Intratracheal bleomycin causes airway remodeling and airflow obstruction in mice. *Exp Lung Res, 38*(3), 135-146. doi:10.3109/01902148.2012.658595
Rajkumar, R., Konishi, K., Richards, T. J., Ishizawar, D. C., Wiechert, A. C., Kaminski, N., & Ahmad, F. (2010). Genomewide RNA expression profiling in lung identifies distinct signatures in idiopathic pulmonary arterial hypertension and secondary pulmonary hypertension. *Am J Physiol Heart Circ Physiol, 298*(4), H1235-1248. doi:10.1152/ajpheart.00254.2009
Ren, S., Johnson, B. G., Kida, Y., Ip, C., Davidson, K. C., Lin, S. L., . . . Duffield, J. S. (2013). LRP-6 is a coreceptor for multiple fibrogenic signaling pathways in pericytes and myofibroblasts that are inhibited by DKK-1. *Proc Natl Acad Sci U S A, 110*(4), 1440-1445. doi:10.1073/pnas.1211179110
Rojas, M., Xu, J., Woods, C. R., Mora, A. L., Spears, W., Roman, J., & Brigham, K. L. (2005). Bone marrow-derived mesenchymal stem cells in repair of the injured lung. *Am J Respir Cell Mol Biol, 33*(2), 145-152. doi:10.1165/rcmb.2004-0330OC
Saito-Diaz, K., Chen, T. W., Wang, X., Thorne, C. A., Wallace, H. A., Page-McCaw, A., & Lee, E. (2013). The way Wnt works: components and mechanism. *Growth Factors, 31*(1), 1-31. doi:10.3109/08977194.2012.752737
Saraswati, S., Alfaro, M. P., Thorne, C. A., Atkinson, J., Lee, E., & Young, P. P. (2010). Pyrvinium, a potent small molecule Wnt inhibitor, promotes wound repair and post-MI cardiac remodeling. *PLoS One, 5*(11), e15521. doi:10.1371/journal.pone.0015521
Scotton, C. J., & Chambers, R. C. (2007). Molecular targets in pulmonary fibrosis: the myofibroblast in focus. *Chest, 132*(4), 1311-1321. doi:10.1378/chest.06-2568
Shtutman, M., Zhurinsky, J., Simcha, I., Albanese, C., D'Amico, M., Pestell, R., & Ben-Ze'ev, A. (1999). The cyclin D1 gene is a target of the beta-catenin/LEF-1 pathway. *Proc Natl Acad Sci U S A, 96*(10), 5522-5527.
Sun, Z., Wang, C., Shi, C., Sun, F., Xu, X., Qian, W., . . . Han, X. (2014). Activated Wnt signaling induces myofibroblast differentiation of mesenchymal stem cells,

contributing to pulmonary fibrosis. *Int J Mol Med, 33*(5), 1097-1109. doi:10.3892/ijmm.2014.1672
Tadjali, M., Zhou, S., Rehg, J., & Sorrentino, B. P. (2006). Prospective isolation of murine hematopoietic stem cells by expression of an Abcg2/GFP allele. *Stem Cells, 24*(6), 1556-1563. doi:10.1634/stemcells.2005-0562
Tetsu, O., & McCormick, F. (1999). Beta-catenin regulates expression of cyclin D1 in colon carcinoma cells. *Nature, 398*(6726), 422-426. doi:10.1038/18884
Thorne, C. A., Hanson, A. J., Schneider, J., Tahinci, E., Orton, D., Cselenyi, C. S., . . . Lee, E. (2010). Small-molecule inhibition of Wnt signaling through activation of casein kinase 1alpha. *Nat Chem Biol, 6*(11), 829-836. doi:10.1038/nchembio.453
van Haaften, T., Byrne, R., Bonnet, S., Rochefort, G. Y., Akabutu, J., Bouchentouf, M., . . . Thebaud, B. (2009). Airway delivery of mesenchymal stem cells prevents arrested alveolar growth in neonatal lung injury in rats. *Am J Respir Crit Care Med, 180*(11), 1131-1142. doi:10.1164/rccm.200902-0179OC
Wang, C., Zhu, H., Sun, Z., Xiang, Z., Ge, Y., Ni, C., . . . Han, X. (2014). Inhibition of Wnt/beta-catenin signaling promotes epithelial differentiation of mesenchymal stem cells and repairs bleomycin-induced lung injury. *Am J Physiol Cell Physiol, 307*(3), C234-244. doi:10.1152/ajpcell.00366.2013
Weidenfeld, J., Shu, W., Zhang, L., Millar, S. E., & Morrisey, E. E. (2002). The WNT7b promoter is regulated by TTF-1, GATA6, and Foxa2 in lung epithelium. *J Biol Chem, 277*(23), 21061-21070. doi:10.1074/jbc.M111702200
West, J. D., Austin, E. D., Gaskill, C., Marriott, S., Baskir, R., Bilousova, G., . . . Majka, S. M. (2014). Identification of a Common Wnt Associated Genetic Signature Across Multiple Cell Types in Pulmonary Arterial Hypertension. *Am J Physiol Cell Physiol*. doi:10.1152/ajpcell.00057.2014
Xu, L., Corcoran, R. B., Welsh, J. W., Pennica, D., & Levine, A. J. (2000). WISP-1 is a Wnt-1- and beta-catenin-responsive oncogene. *Genes Dev, 14*(5), 585-595.
Yan, D., Wiesmann, M., Rohan, M., Chan, V., Jefferson, A. B., Guo, L., . . . Williams, L. T. (2001). Elevated expression of axin2 and hnkd mRNA provides evidence that Wnt/beta -catenin signaling is activated in human colon tumors. *Proc Natl Acad Sci U S A, 98*(26), 14973-14978. doi:10.1073/pnas.261574498
Yang, Y. C., Zhang, N., Van Crombruggen, K., Hu, G. H., Hong, S. L., & Bachert, C. (2012). Transforming growth factor-beta1 in inflammatory airway disease: a key for understanding inflammation and remodeling. *Allergy, 67*(10), 1193-1202. doi:10.1111/j.1398-9995.2012.02880.x
Zhang, M., Shi, J., Huang, Y., & Lai, L. (2012). Expression of canonical WNT/beta-CATENIN signaling components in the developing human lung. *BMC Dev Biol, 12*, 21. doi:10.1186/1471-213X-12-21

CHAPTER III: DYRK2 ENHANCES WNT SIGNALING ACTIVATION THROUGH GSK3β DIRECTED PHOSPHORYLATION OF LRP6

Wnt signaling is an evolutionarily conserved signaling pathway that regulates development and is misregulated in cancer formation (Saito-Diaz et al., 2013). Activation of Wnt signaling is dependent on the cytoplasmic steady-state level of the transcriptional co-activator, β-catenin. Cytoplasmic β-catenin is continually synthesized and degraded by a destruction complex consisting of the scaffolding proteins Axin and adenomatous polyposis coli (APC) as well as the kinases casein kinase 1α (CK1α) and glycogen synthase kinase-3 β (GSK3β). CK1α phosphorylates β-catenin, priming β-catenin for additional phosphorylation by GSK3β (Saito-Diaz et al., 2013). These phosphorylation events target β-catenin for proteasomal degradation to maintain its low levels in the cytoplasm. When a Wnt ligand binds to the co-receptors Fzd and LRP5/6, in a process that has not been well established, the intracellular domain of LRP5/6 (LRP5/6 ICD) is phosphorylated at multiple sites by CK1 and GSK3. Phosphorylation of LRP5/6 ICD promotes the binding of Axin to LRP5/6 ICD, and recruits other components of the destruction complex to the membrane, thereby preventing the phosphorylation of β-catenin within the destruction complex and blocking its degradation. Unphosphorylated β-catenin builds up in the cytoplasm, translocates to the nucleus and then binds to the transcriptional factor TCF/LEF1 to initiate a Wnt-specific transcriptional program (Saito-Diaz et al., 2013). Because phosphorylation plays in key role in Wnt signaling regulation, the Lee lab was interested in identifying novel kinases that regulate the Wnt signaling pathway.

To identify new kinases in the Wnt signaling pathway, we employed a genome-scale expression cloning using the *Xenopus laevis* axis duplication assay as a readout. Maternal β-catenin is the dorsalizing factor in *Xenopus laevis* (Funayama, Fagotto, McCrea, & Gumbiner, 1995). mRNAs corresponding to activators of Wnt signaling, when injected into the ventral side of early stage embryos, induce secondary dorsal structures, whereas mRNAs corresponding to inhibitors, when injected in the dorsal side of early stage embryos, block dorsalization. The identification of many Wnt components have been revealed through this assay, including GSK3 and LRP5/6, which induce ventralization and dorsalization respectively (He, Saint-Jeannet, Woodgett, Varmus, & Dawid, 1995; Tahinci et al., 2007; Tamai et al., 2000). We injected mRNA encoding human kinase genes upstream of a polyadenylation sequence into embryos and identified several potential activators of Wnt signaling based on their dorsalization ability. The mRNA was generated from a kinase library using successive rounds of PCR to fuse separate oligonucleotides into a single mRNA fragment. One of the more potent kinases identified was DYRK2.

Dual specificity tyrosine-regulated kinases (DYRKs) are an evolutionarily conserved subfamily of kinases that belong to the CMGC group of kinases, a group that also includes MAPK and GSK3 (Aranda, Laguna, & de la Luna, 2011). The DYRK subfamily is further divided into three branches: YAKs, DYRK1s and DYRK2s. Only DYRK1 and DYRK2 branches exist in mammals and consists of five members: DYRK1A, DYRK1B, DYRK2, DYRK3, and DYRK4. Protein conservation within the kinase domain of DYRKs divides the family into the the DYRK1 branch (DYRK1A and DYRK1B) and the DYRK2 branch (DYRK2, DYRK3, and DYRK4) (Aranda et al., 2011).

All DYRKs contain a tyrosine site that must be phosphorylated to achieve full kinase activity. In addition, DYRK2/3/4 contain an N-terminal region essential for autophosphorylation (known as NAPA) whereas DYRK1A/B are phosphorylated by an unknown kinase (Aranda et al., 2011). DYRKs regulate a variety of cell processes, including cell survival, cell differentiation, and gene transcription (Aranda et al., 2011). DYRK2 also regulates many processes involving GSK3 by priming substrates for subsequent GSK3 phosphorylation, as in the case of CRMP4, eIF2Bε, NFAT, Tau, Snail, cJun, and cMyc (Aranda et al., 2011). Herein, we now report the identification of DYRK2 as a regulator of Wnt signaling via its regulation of LRP6 phosphorylation by GSK3.

Methods

Xenopus laevis Axis Duplication Assay and Developmental Screen

Xenopus laevis embryos were fertilized and processed as previously described (Tahinci et al., 2007). Briefly, *Xenopus* adult females are injected with 1 mL human chorionic gonadotrophin (HCG). 24 hours later, eggs are collected in 1x Modified Barth's Saline (MBS; 88mM NaCl, 1mM CaCl2, 1 mP MgSO4, 5 mM HEPES, 2.5 mM NaHCO3) + gentamycin and fertilized *in vitro* using excised testes from *Xenopus* adult males. Fertilized eggs are then dejelleyed by incubating in 2% cysteine (pH 7.7) followed by rinsing with 0.1 Marc's modified Ringer's (MMR) solution (0.1 NaCl, 2 mM KCl, 1 mM $MgSO_4$, 2 mM $CaCl_2$, 5 mM HEPES pH 7.8, 0.1 mM EDTA). Dejelleyed embryos were injected at the 4-cell stage in 1/3 MMR + Ficoll (4%) using a microinjector and then transferred to 1x MMR solution. Embryos are allowed to develop at room temp for 48 hours prior to fixation in 3.7% formaldehyde in 1x MBS for 24 hours.

Generation of mRNAs

cDNA corresponding to 232 human kinases from the Harvard Institute of Proteomics (HIP) FLEXgene human kinase cDNA collection (pDNR-Dual complete set; https://plasmid.med.harvard.edu/PLASMID/GetCollectionList.do) were amplified by PCR using the primer set (5' oligo sequence: GGCCCGCGCGCCAAACGAATGGTC and 3' oligo sequence: CCAAGCCTTCTAATACGACTCACTATAGGGAGACAGTGAG

CGAGGAAGCGGCCGC). To generate an oligonucleotide encoding human kinases upstream of a CS2 Poly(A) fragment, a PCR-amplified fragment of the pCS2 Poly(A) sequence was generated (5' oligo sequence: GACCATTCGTTTGGCGCGCGGGCCTGAGATCCAGACATGATAAGATAC; 3' oligo sequence: GAATTAAAAAACCTCCCACACCTCCCCCTGAACCTG). The two fragments were "sewn" together in a third PCR reaction to generate an oligonucleotide containing human kinase cDNA upstream of a CS2 Poly(A) sequence. These fragments were then converted to capped mRNA using mMessage mMachine (Ambion) prior to injection into embryos.

Luciferase assay

HEK293 STF cells were plated at a concentration of $5X10^5$ cells/well in a 12-well plate for 24 hours using DMEM + 8% FBS. To analyze luciferase activation, culture media was removed and HEK293 STF cells were incubated with vigorous shaking in 1x Passive Lysis Buffer (Biotium) for 15 min. 45μl of the lysed solution were then incubated with 45μl of Steady-Glo (Promega) and luciferase activity analyzed. Luciferase

activation was normalized to CellTiter-Glo Assay (Promega). While all experiments were performed in triplicates and averaged, representative data is provided.

Immunoblotting

HEK293 STF cells were plated at a concentration of $5X10^5$ cells/well in a 6-well plate for 24 hours. Cells were lysed by incubating on ice in 15 minutes in lysis buffer (10 mM H-EPES [pH 7.8], 10 mM KCl, 2 mM $MgCl_2$, 0.1 EDTA, 1x PMSF, 1x LPA, 1x PhosSTOP [Sigma], 1x Sodium Flouride), scraped, transferred to microcentrifuge tubes and NP-40 was added (0.5%). Lysates were vortexed for 30 sec, sheared through a 23-G needle, then centrifuged for 3 min at 13,000xg. Supernatants were recovered and mixed with Sample Buffer. Lysates were separated through SDS-PAGE electrophoresis and transferred to a nitrocellulose membrane. Membranes were incubated with horseradish peroxidase-conjugated secondary antibodies and imaged with SuperSignal West Pico or Femto Chemiluminescent Substrate (Pierce) using the C-DiGit Blot Scanner (Li-COR).

Antibodies used include β-catenin (1:1000; BD Transduction), total LRP6 (1:1000; CST), pLRP6 (1:1000; Millipore), GAPDH (1:1000; Santa Cruz), cMYC (1:1000; Vanderbilt Antibody Core), VSVG (1:1000; Bethyl Laboratories), and MBP (1:1000; Vanderbilt Antibody Core).

Plasmids and mRNA generation

hDYRK2 and hDYRK1α were subcloned into the pCS2 plasmid using Gibson assembly (New England Biolabs). hDYRK2 was also subcloned into MYC-pCS2 using Gibson assembly to generate MYC-DYRK2. VSVG-LRP6 and MBP-GSK3 constructs were described previously (Jernigan et al., 2010). The K251R kinase dead version of MYC-

DYRK2 was generated by using the QuikChange Site Directed Mutagenesis Kit (Agilent) with the following primers: Fw-CATTCCGCACCATCCTTAGGGCCACGTGCTG, Rv-CAGCACGTGGCCCTAAGGATGGTGCGGAATG. This converts a lysine to arginine at the ATP binding site of MYC-DYRK2. GST-DYRK2 was generated by subcloning hDYRK2 into the pGEX vector using restriction cloning. mRNA was generated using mMessage mMachine (Ambion) and purified using RNA Cleanup columns (Qiagen).

Protein Purification

Recombinant GSK3β was obtained from a commercial source (New England Biolabs). LRP6-ICD was purified as described previously (Cselenyi et al., 2008). hDYRK2 was purified by growing BL21 cells inoculated with GST-hDYRK2 to an OD_{600} of 37°C and induced with IPTG (1 μg/mL) for 4 hours. Induced bacteria was harvested, sonicated and hDYRK2 protein was purified on glutathione resin. Eluted protein was dialyzed into 20mM Tris pH 7.4, 1mM DTT, flash frozen, and stored at -80°C.

Morpholino generation

A translation blocking morpholino against xDYRK2's 5' UTR (TTGGGAAGGCATACCCAGTAACTCA) was designed and ordered through Gene Tool, LLC.

Co- immunoprecipitation

HEK293 STF cells were seeded into 10cm plates a concentration of $1x10^6$ cells/ml. After 48 hours, cells were lysed in Non-Denaturing Lysis Buffer (NDLB, 1% Triton X-100, 50 mM Tris pH7.4, 300 mM NaCl, 5 mM EDTA, 0.02% Sodium Azide, 0.1% LPA, 1x PMSF) for 15 minutes on ice. Cells were then scraped, vortexed, centrifuged and the

resulting supernatant was flash frozen and stored at -80°C. 500 μg protein lysates were than thawed and precleared with 25 μl Protein G Sepharose 4 Fast Flow beads (GE Healthcare) for 30 min. The beads were removed via centrifugation, 1 μg of antibody was added to the supernatant and the lysates were shaken for 1 hour at 4°C. 25 μl additional Protein G Sepharose 4 Fast Flow beads were added and the lysates were shaken for another hour at 4°C. The lysates were then washed, centrifuged to remove the supernatant, and the resulting beads were combined with sample buffer and boiled for 15 min to separate the isolated protein from the beads.

Kinase assays

Kinase assays using 2 mM ATP (Sigma) or 2 mM ATP [γ-^{32}P] (PerkinElmer) were performed as follows: purified LRP6-ICD (200 nM), recombinant GSK3β (200 nM) and 1x Protein Kinase Buffer (NEB) were combined with or without purified hDYRK2 in the presence of ATP or ATP [γ-^{32}P] for 20 minutes at 35°C. Sample Buffer was added, and samples processed for SDS-PAGE/immunoblotting.

Results

hDYRK2 activates the Wnt signaling pathway. Many components of the Wnt signaling pathway are phosphorylated as a means of pathway regulation. Despite the importance of these phosphorylation events, only five kinases have been identified as targeting core components of the Wnt signaling pathway (GSK3, CK1, PIP5KI, HIPK, and NLK) (Verheyen & Gottardi, 2010). To identify novel kinases that affect the Wnt signaling pathway, mRNA corresponding to 232 human kinases from the the Harvard Institute of Proteomics (HIP) FLEXgene human kinase cDNA collection were injected

into four-cell stage *Xenopus laevis* embryos in 29 pools containing 8 separate human kinase mRNAs. mRNA was generated using successive rounds of PCR to generate a single oligonucleotide containing human kinase coding sequence upstream of a polyadenylation site (Fig. 1). mRNAs from pools that affected development were then individually injected into embryos to identify the kinase of interest. hDYRK2 mRNA injection affected head and trunk formation in *Xenopus* embryos at mRNA below 1 ng (data not shown), indicating that hDYRK2 might regulate dorsalization/Wnt signaling. To provide further confirmation that hDYRK2 regulates Wnt signaling, we injected hDYRK2 mRNA into the ventral blastomere of 4-8 cell stage *Xenopus laevis* embryos. I observed secondary axis formation after injecting embryos with hDYRK2 mRNA (Fig. 2A). As secondary axis formation in *Xenopus laevis* embryos is characteristic of inappropriate activation of Wnt signaling in ventral blastomeres, these results suggest that hDYRK2 interacts with the Wnt signaling pathway (Funayama et al., 1995; McMahon & Moon, 1989).

I next wanted to confirm that hDYRK2 affected the Wnt signaling pathway by increasing transcription of Wnt target genes. Using a cell line containing a stably transfected, luciferase-based Wnt reporter (HEK293 STF), I found that only hDYRK2 transfected in combination with recombinant Wnt3a treatment significantly increased luciferase levels when compared to recombinant Wnt3a alone (Fig. 2B). The phosphorylate of LRP6 can be monitored using an antiphospho-LRP6 antibody (Tamai et al., 2004). hDYRK2 transfection increased p-LRP6 protein expression but increased intracellular β-catenin protein levels was only observable when hDYRK2 transfection was combined with the addition of recombinant Wnt3a (Fig. 2B). Thus, hDYRK2

enhances LRP6 phosphorylation and synergizes with Wnt3a to activate Wnt gene transcription.

hDYRK2's catalytic activity regulates its interaction with the Wnt signaling and is unique in the DYRK kinase family. Once I established that hDYRK2 synergizes with Wnt3a to activate the Wnt transcriptional response, I tested whether this activity was specific to hDYRK2 or was shared by other kinases in the DYRK subfamily. I chose DYRK1A as comparison for DYRK2 because DYRK1A and DYRK2 differ greatly in terms of structure and are localized to different cellular compartments (Aranda et al., 2011). I found that hDYRK1A did not increase luciferase activity in HEK293 STF cells by itself or in combination with Wnt3a treatment (Fig. 3A). In addition, hDYRK1A mRNA did not induce duplications to the same extent as hDYRK2 mRNA (3.55% DYRK1A duplications vs. 66.25% DYRK2 duplications) when injected into *Xenopus* embryos (Fig. 3B). These data suggest that DYRK enhancement of Wnt signaling is specific to DYRK2.

I next tested if DYRK2's enhancement was due to its catalytic activity as DYRK2 also acts as a protein scaffold for the EDVP E3 ligase complex, which contains the proteins EDD, DDB1, and VPRBP (Maddika & Chen, 2009). While the EDVP E3 ligase complex ubiquitinates katanin 60 and requires the the presence of DYRK2 to form, DYRK2's kinase activity is dispensable for this ubiquitination (Maddika & Chen, 2009). To determine whether the catalytic or scaffolding activity of DYRK2 was essential for its activity in the Wnt pathway, I generated a mutant of DYRK2 (lysine at codon 251 changed to an arginine or K251R), which prevents the binding of ATP to hDYRK2 (Perez et al., 2012). This DYRK2 K251R mutant has been previously characterized as a

"kinase dead" version of DYRK2 (Perez et al., 2012). I found that DYRK2 K251R, in contrast to wild type DYRK2, did not enhance Wnt3a activation in HEK293 STF cells (Fig 3B). Hence, DYRK2's catalytic activity is required for its enhancement ability. Furthermore, I found that DYRK2 K251R did not significantly inhibit Wnt3a-mediated activation, indicating that the DYRK2 K251R mutant does not act in a dominant negative fashion (Fig 3B).

hDYRK2 is required for Wnt activation during *Xenopus* embryo development. To determine if DYRK2 is required for Wnt signaling, I tested whether a small molecule inhibiter of DYRK activation, INDY, could inhibit Wnt activation (Ogawa et al., 2010). INDY inhibits DYRK activity by binding to the ATP binding cleft of DYRKs. I found that INDY treatment significantly decreased Wnt3a induced luciferase activation in HEK293 STF cells albeit not to basal levels (Fig 4A). I next tested whether there is an *in vivo* requirement of DYRK2 by injecting a translation blocking morpholino (xDYRK2 MO) into both cells of 2 cell-stage *Xenopus* embryos. I found that xDYRK2 MO injection induces posteriorization in embryos that can be rescued with hDYRK2 mRNA injection (Fig 4A). The observed posteriorization phenotype is consistent with Wnt inhibition pre-midblastula transition (MBT) (Saito-Diaz et al., 2013). These results indicate that DYRK2 is required for Wnt activation during early *Xenopus* development.

hDYRK2 enhances the catalytic activity of GSK3. An increase in pLRP6 expression suggested that DYRK2 interacted with membrane components of the Wnt pathway. Previous studies found that DYRK enhanced GSK3 phosphorylation of the human microtubule-associated protein tau, suggesting that the two kinases may interact (Woods et al., 2001). I repeated this assay and confirmed that DYRK2 not only

phosphorylates tau but also increases phosphorylation of tau when co-incubated with GSK3 (Fig 5A). It also appears that both GSK3 and DYRK2 have increased levels of phosphorylation when combined, raising the possibility that these kinases co-phosphorylate to increase their respective phosphorylation ability (Fig 5A). The addition of LiCl in this assay not only inhibited GSK3 activity but also the activity of DYRK2 as well (Fig 5A). To determine whether DYRK2 enhances the capacity of GSK3 to phosphorylate LRP6 in vitro, I incubated recombinant DYRK2, GSK3, and the intracellular domain of LRP6 (Cselenyi et al., 2008) in a kinase reaction and immunoblotted for phospho-LRP6 (ser1490). I found that the addition of DYRK2 enhances the phosphorylation of LRP6 on ser1490 (Fig 5B). To determine if DYRK2 or GSK3 was responsible for increased ser1490 phosphorylation on LRP6, I conducted a similar kinase assay using radiolabeled ATP. I found by autoradiography that DYRK2 enhanced the radiolabel incorporation of 32P into LRP6 ICD and that DYRK2 itself was able to phosphorylate LRP6 ICD directly (lane 4 and lane 7, Fig 5C). These studies suggest that DYRK2 directly phosphorylates LRP6 and enhances the capacity of GSK3 to phosphorylate LRP6. However, it is important to note that an unknown phosphorylated product appears when DYRK2 and GSK3 are combined (lane 2, lowest band, Fig 5C). Unfortunately, this band is at the same size as the phosphorylated LRP6 ICD, making it difficult to compare GSK3 phosphorylated LRP6 ICD to DYRK2+GSK3 phosphorylated LRP6 ICD (lane 4 vs. lane 7) as some of the expression in the latter case likely originates from the unknown phosphorylated product. Due to this unknown product, this last piece of data is preliminary.

hDYRK2 binds to GSK3 but not to LRP6. To test whether DYRK2, LRP6, and GSK3 interact, I performed co-immunoprecipitation (CoIP) experiments with MYC-tagged DYRK2, VSVG-tagged LRP6, and MBP tagged GSK3 in HEK293 STF cells. I found that hDYRK2 CoIPs with MBP-tagged GSK3 (Fig 6A) but not with LRP6 (Fig 6B). Thus, DYRK2 binds to GSK3 and not LRP6 in these preliminary studies.

Discussion

My results suggest that DYRK2 enhances Wnt signaling pathway activation by promoting LRP6 phosphorylation (hence activation) via regulation of GSK3 enzymatic activity (Fig 6C). My evidence that DYRK2 regulates the Wnt pathway comes from our demonstration that DYRK2 1) induces *Xenopus* axis duplication, 2) promotes Wnt reporter activity, 3) increases intracellular β-catenin levels, and 4) promotes phosphorylation. My morpholino studies in *Xenopus* embryos and small molecule inhibitor studies in cultured cells suggest a requirement for DYRK activity *in vivo* and in cultured cells. Finally, I provide mechanistic evidence that DYRK2 promote Wnt signaling by binding to GSK3 and enhancing its activity towards LRP6 as well as a model of this interaction.

GSK3 regulation: the black box of Wnt signaling

GSK3 is a major component of the Wnt signaling pathway, and several elements of its regulation remain unclear. For example, it is unknown how binding of a Wnt ligand to the co-receptors Fzd and LRP5/6 induces GSK3 to phosphorylate LRP5/6 or how GSK3 alternates between membrane activation of LRP6 and cytoplasmic regulation of β-catenin. GSK3 is a kinase with a large number of substrates and GSK3 catalytic activity is regulated by “priming” phosphorylation events that occur on GSK3 substrates

by other kinases and phosphorylation of GSK3 by other kinases (Beurel, Grieco, & Jope, 2015). In the former case, substrates of GSK3 are often primed at 4 residues C-terminal to a S/T site on the substrate targeted by GSK3 (S/T-X-X-X-S/T(P)) (Beurel et al., 2015; Wu et al., 2009). Priming a substrate in this manner is important for efficient GSK3 phosphorylation because it shifts the N-terminal S/T site on the substrate from being displaced from the kinase domain on GSK3 to being adjacent to the kinase domain on GSK3 (Beurel et al., 2015; ter Haar et al., 2001). In the latter case, phosphorylation of GSK3 by other kinases can inhibit or promote GSK3's catalytic activity. One example of inhibitory phosphorylation of GSK3 is phosphorylation on GSK3 at Ser 9. GSK3 is named for its substrate in the insulin signaling pathway, glycogen synthase. Insulin induces AKT to phosphorylate GSK3 at Ser 9 (ter Haar et al., 2001). Phosphorylation of Ser 9 induces a conformational change in GSK3, shifting the N-terminal portion of GSK3 closer to the kinase domain and preventing substrates from accessing this domain (Beurel et al., 2015; ter Haar et al., 2001). An example of activating phosphorylation of GSK3 is phosphorylation of GSK3 at Tyr 216, which dramatically increases the catalytic activity of GSK3 by inducing a conformational change in GSK3 that exposes the substrate binding groove of GSK3 (Beurel et al., 2015; Gao et al., 2015; Hanks & Hunter, 1995; ter Haar et al., 2001). Thus, phosphorylation at Ser 9 and Tyr 216 demonstrate that GSK3's catalytic activity can be regulated by other kinases.

The relationship between GSK3 phosphorylation state and Wnt signaling has not been well characterized. Whereas Ser 9 phosphorylation inhibits GSK3's capacity to phosphorylate other substrates, Ser 9 phosphorylation does not affect GSK3's capacity

to phosphorylate of β-catenin (Ng et al., 2009; Voskas, Ling, & Woodgett, 2010). Phosphorylation of Tyr 216 by FAK/PYK2 on GSK3 has been shown to promote accumulation of cytoplasmic β-catenin but paradoxically does not affect GSK3's capacity to phosphorylate β-catenin. It was subsequently shown that phosphorylation at Tyr 216 on GSK3 induces mono-ubiquitylation of GSK3 by the E3 ligase β-TrCP and that mono-ubiquitylated GSK3 prevents proteasomal degradation of β-catenin via an unknown mechanism (Gao et al., 2015). My own study indicates that DYRK2 phosphorylates GSK3 to promote its kinase activity, and DYRK2 activity on GSK3 represents a previously unappreciated mechanism by which GSK3 activity can be regulated.

DYRK1A has opposing effects compared to DYRK2

DYRK1A has been shown to phosphorylate GSK3 and regulate its activity (Campbell & Proud, 2002; Song et al., 2015). DYRK1A binds and phosphorylates GSK3 at Thr356, which inhibits the capacity of GSK3 to phosphorylate its substrates (Song et al., 2015). The reason for the differing activities of DYRK1A and DYRK2 may be due to differences of these kinases outside their catalytic regions (Aranda et al., 2011). Indeed, DYRK2 and DYRK1A have differing requirements for substrate binding (Campbell & Proud, 2002). These studies indicate that different DYRK family members are different not only in structure and substrate preference, but also how DYRK may regulate the activity of a common substrate.

DYRK2 in Cancer

Several studies indicate that DYRK2 is associated with the incidence and aggressiveness of breast, esophageal and lung cancers. However, there are conflicting

reports as to whether DYRK2 acts in a positive or negative fashion. DYRK2 was identified as the most highly expressed gene among 15 identified in the 12q13-q14 chromosome region of esophageal and lung adenocarcinomas (Miller et al., 2003). In addition, microarray analysis revealed that almost 20% of lung adenocarcinomas included in this study had an overexpression of DYRK2 mRNA (Miller et al., 2003). In contrast, several studies have reported a correlation between a decrease in DYRK2 expression and an increase in cancer incidence and invasiveness. In these studies, DYRK2 targets substrates for degradation in order to regulate cell cycle control and cellular migration (Mimoto et al., 2013; Perez et al., 2012; Taira et al., 2012). Specifically, DYRK2 primes Snail, cJun and cMyc for GSK3-directed degradation. Knockdown of DYRK2 correlates with increases in Snail, cJun and cMyc levels (Mimoto et al., 2013; Perez et al., 2012; Taira et al., 2012). Furthermore, increased Snail levels due to DYRK2 knockdown promoted invasiveness in a mouse xenograft model, and patients with tumors that express low levels of DYRK2 have a higher rate of cancer recurrence (Mimoto et al., 2013). Similarly, increased cJun and cMyc levels via DYRK2 knockdown increased tumor size and invasiveness in mouse xenograft models, and decreased DYRK2 expression correlates with enhanced invasiveness of breast cancer tumors (Taira et al., 2012). DYRK2 may also be regulated in tumors. SIAH, an E3 ligase, has been shown to target DYRK2 for ubiquitin-mediated degradation under hypoxic conditions. Decreased DYRK2 levels result in its decreased phosphorylation of the tumor suppressor p53, a key initiating step in p53 directed apoptosis (Perez et al., 2012). SIAH's regulation of DYRK2 in hypoxic conditions provide a potential mechanism for cancer cells in hypoxic conditions to evade chemotherapy initiated apoptosis (Perez

et al., 2012). Thus, DYRK2 affects cancer invasiveness, incidence and response to treatment by either regulating its substrate's activity via proteolysis or phosphorylation. My data indicates that DYRK2 interacts with the Wnt signaling pathway through the latter mechanism to promote signaling. There is emerging evidence that the Wnt pathway represents an oncogenic pathway that plays critical roles in nearly all major human cancers. Thus, further studies to more fully define the role of DYRK2 in the Wnt pathway may provide insight into the treatment of these devastating diseases.

*This work was performed in the lab of Dr. Ethan Lee. Dr. Emilios Tahinci, Dr. Chris Cselenyi, Leif Neitzel, and Emily Crispi contributed to this work.

Figures

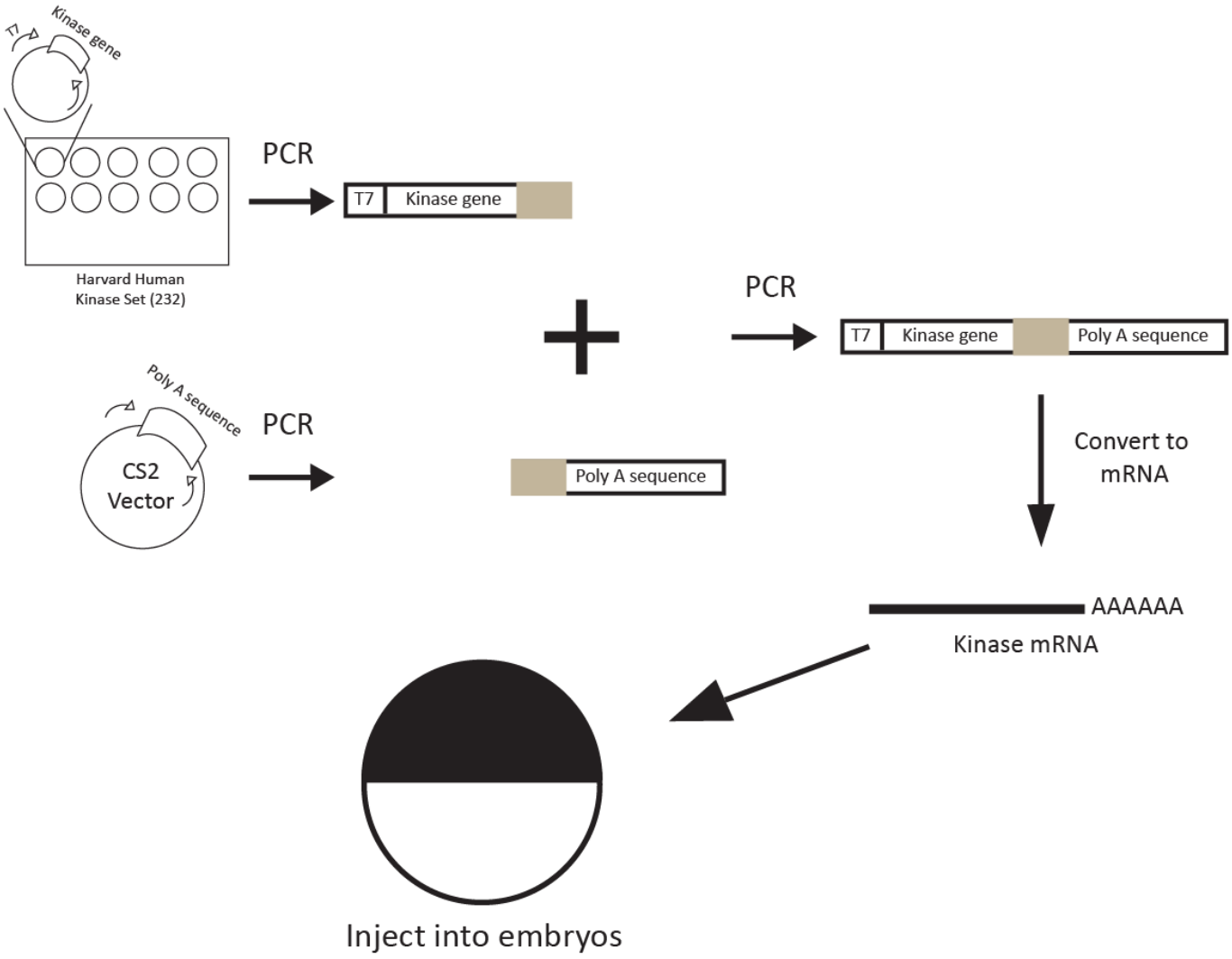

Figure 1 Design of *Xenopus* developmental screen. cDNA encoding 232 separate kinases and the CS2 Poly (A) sequence was amplified using PCR and then fused through successive PCR. The corresponding cDNA fragment was then converted into mRNA and injected into 4-cell stage *Xenopus* embryos.

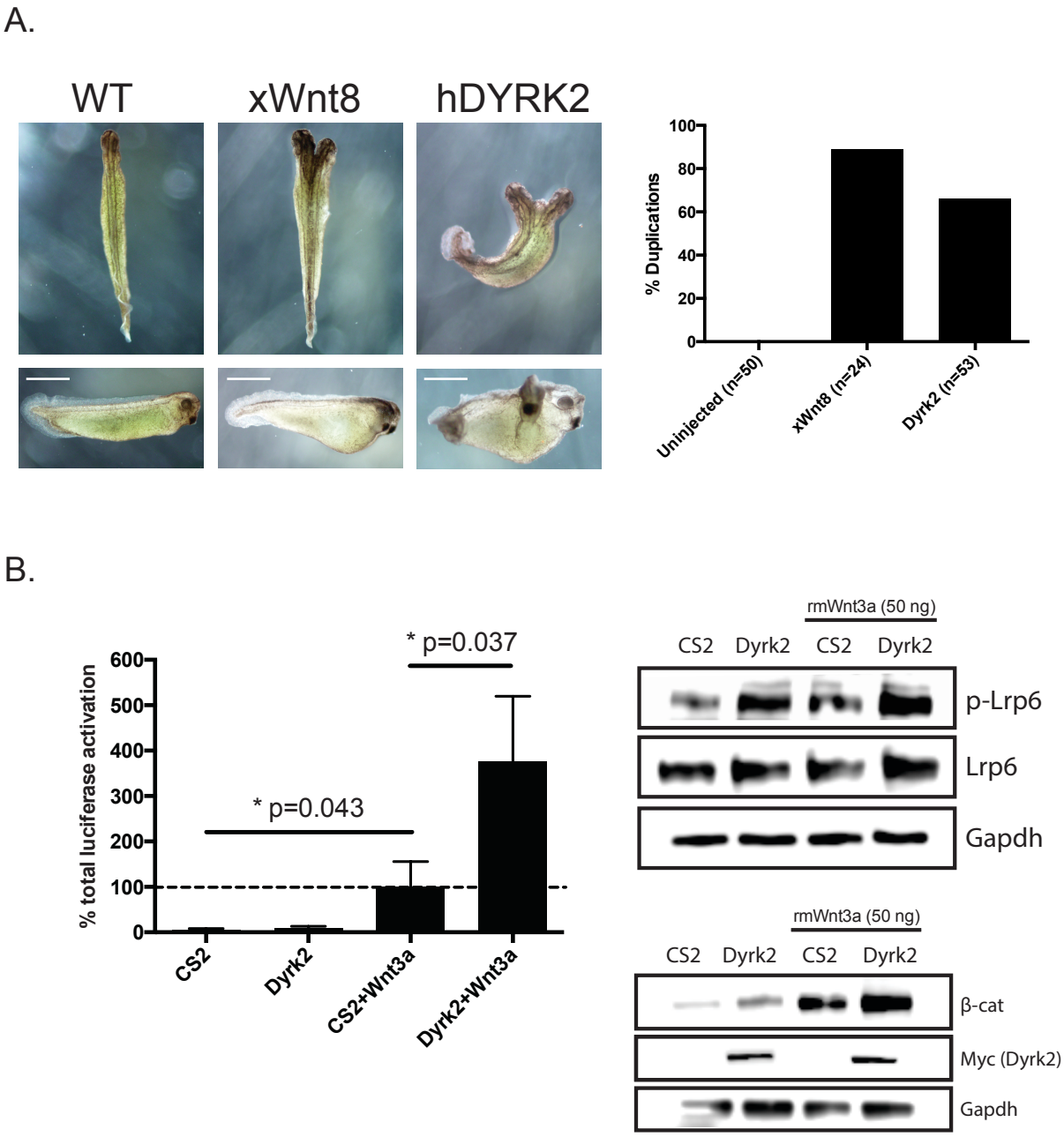

Figure 2 hDYRK2 activates the Wnt signaling pathway. **A)** hDYRK2 mRNA injection into ventral blastomeres of 4-8 cell *Xenopus* embryos induce axis duplication. Quantification shown at right. Both partial and full duplications included. Scale bar = 1 mm. Results are cumulative for two independent experiments. **B)** Luciferase activation in HEK cell lines containing a Wnt-activated luciferase reporting system (HEKSTF). HEKSTF cells were transfected with or without a plasmid containing hDYRK2 and treated with rmWnt3a (50 ng) for 24 hours. Increases in LRP6 phosphorylation and intracellular β-catenin shown in Western blots at right. Results are representative of two independent experiments.

A.

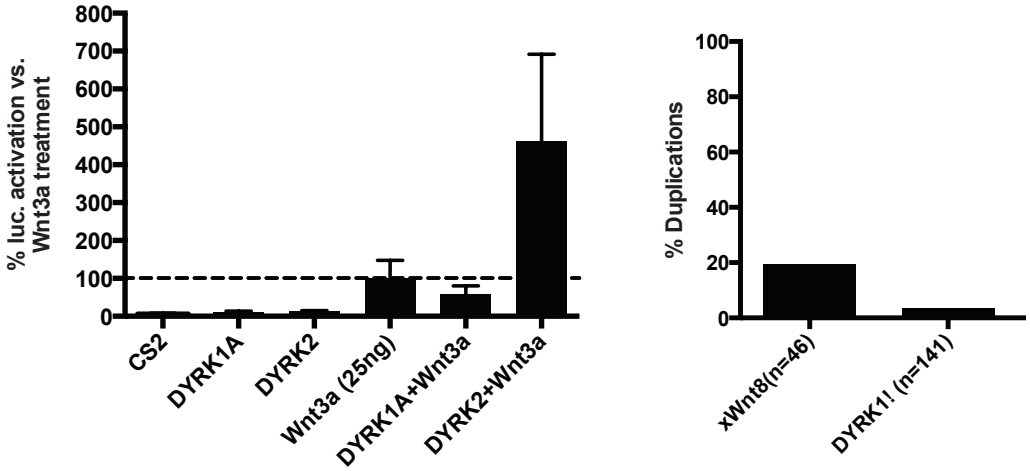

B.

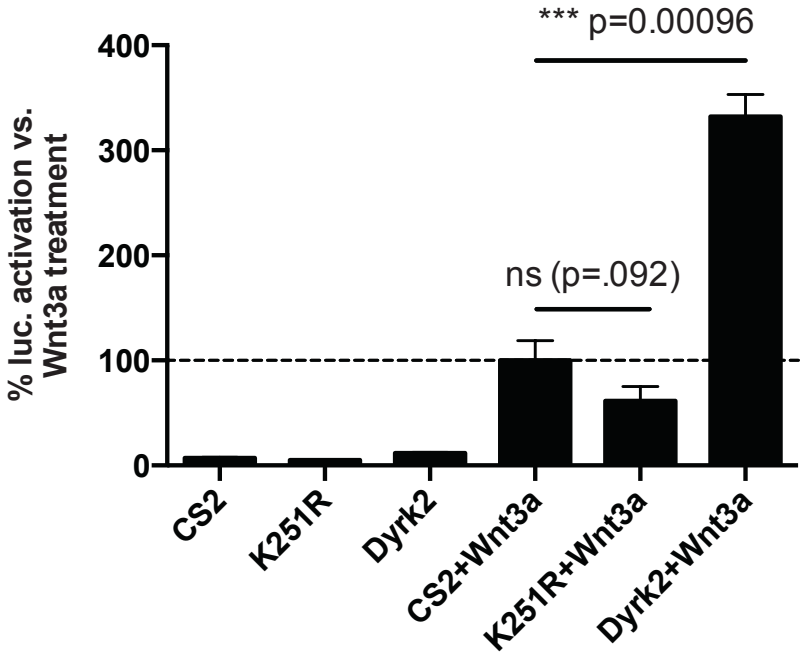

Figure 3 hDYRK2 enhances Wnt signaling transduction compared to other hDYRK family members and hDYRK2's catalytic activity is required for this enhancement. **A)** Luciferase activation in HEKSTF cells treated with rmWnt3a (25 ng) and co-transfected with plasmid containing DYRK family member hDYRK1A or hDYRK2 gene coding sequence. Results are representative of two independent experiments. **B)** Percentage of *Xenopus* embryos resulting in full or partial secondary axis formation after injection of xWnt8 (.5 ng) and hDYRK1A mRNA (2 ng) individually or in combination. **C)** Luciferase activation in HEKSTF cells transfected with the catalytically inactive form of hDYRK2 (K251R) and rmWnt3a (25 ng) individually or in combination. Results are representative of five independent experiments.

A.

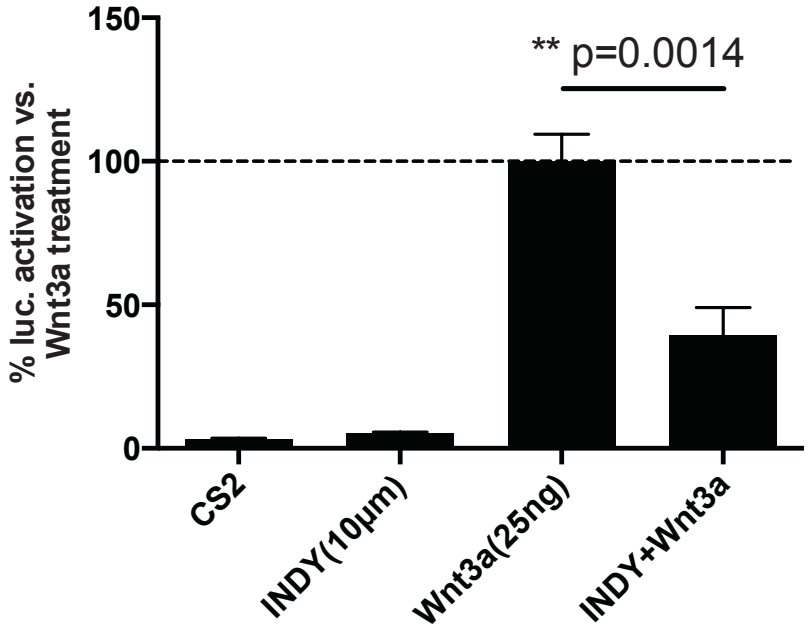

B.

Figure 4. hDYRK2 is important but not required for Wnt activation *in vitro* and in *Xenopus* embryo development. **A)** Luciferase activation in HEKSTF cells co-treated with rmWnt3a (25 ng) and the DYRK family inhibitor (INDY; 10 μM) for 24 hours. Western blots of intracellular β-catenin shown at right. DMSO treatment was used as a control treatment in non-INDY treated cells. Results are representative of three independent experiments. **B)** A morpholino targeting xDYRK2 translation injected into both blastomeres of a 2-cell stage *Xenopus* embryo (20 ng) induces posteriorization that can be rescued by hDYRK2 mRNA. Scale bar = 1 mm.

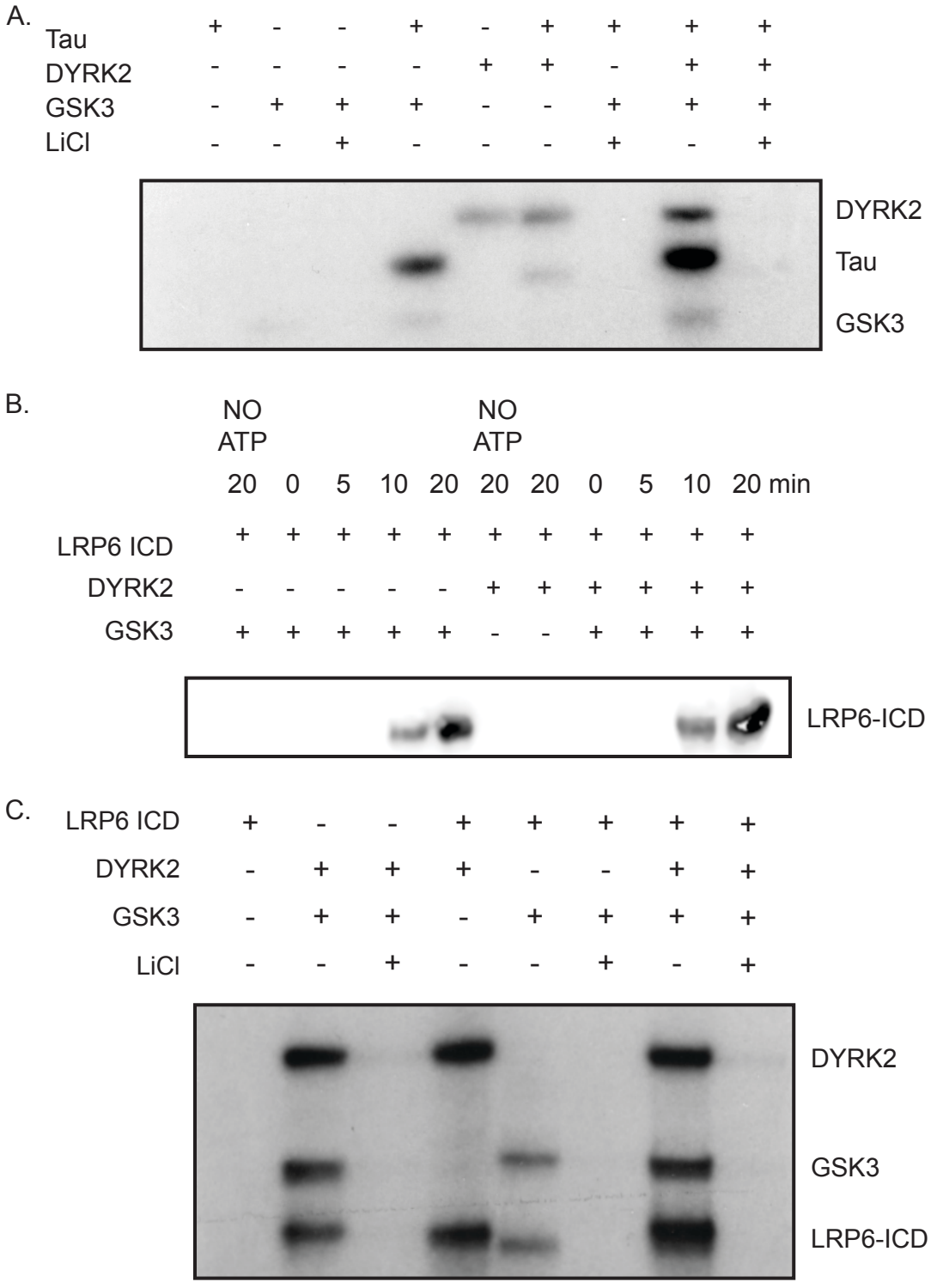

Figure 5. hDYRK2 enhances the catalytic activity of GSK3. **A)** Autoradiograph after incubation of different combinations of ATP^{32} (2mM) and purified Tau (300nM), hDYRK2-GST (300nM), GSK3 (300nM), or LiCl (100 mM). **B)** phospho-LRP6 expression via western blotting after incubation of different combinations of ATP (2mM) and purified LRP6 (300nM), hDYRK2-GST (300nM), or GSK3-HA (300nM). **C)** Autoradiograph after incubation of different combinations of ATP^{32} (2mM) and purified LRP6 (300nM), hDYRK2-GST (300nM), or GSK3-HA (300nM).

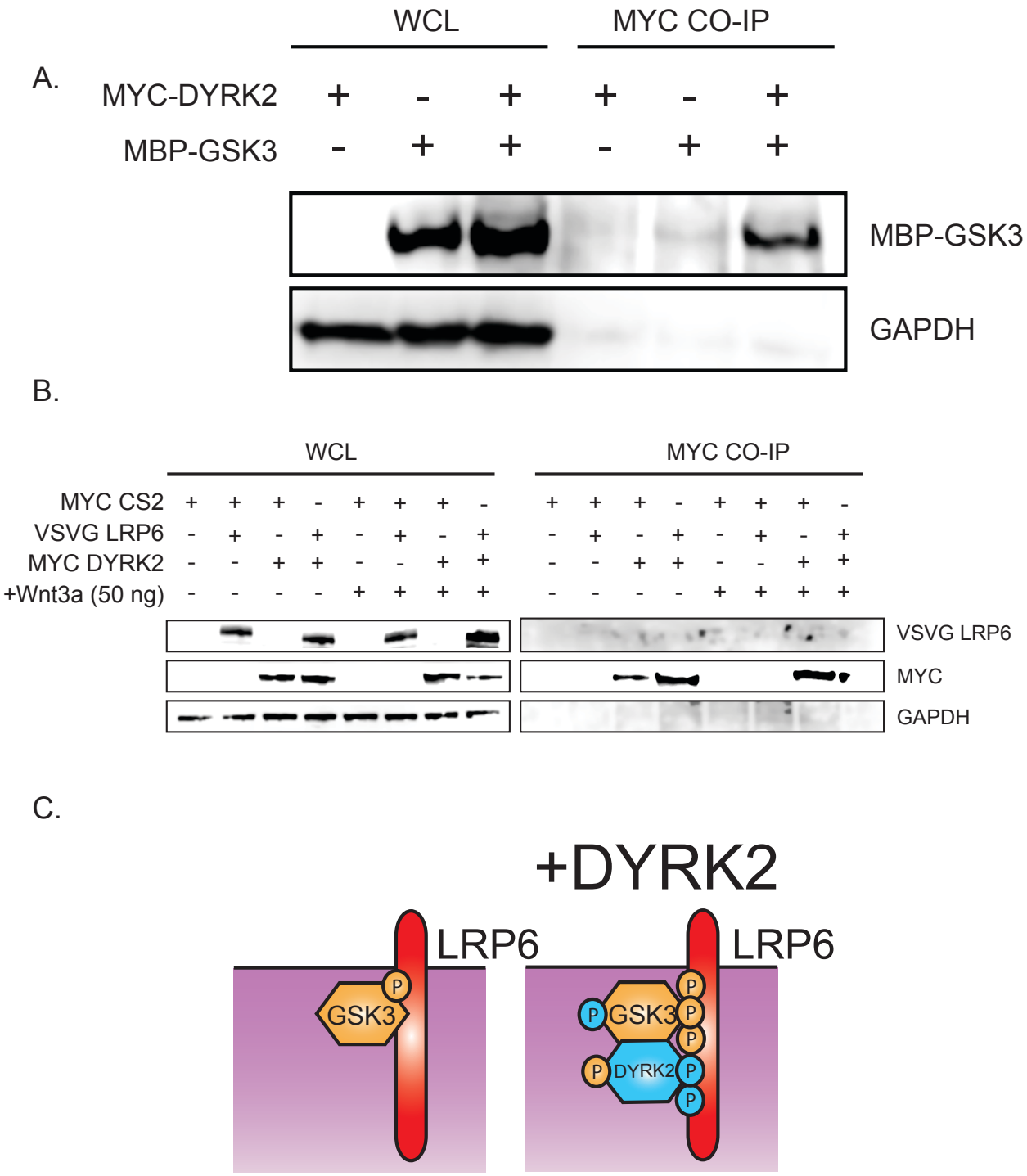

Figure 6. hDYRK2 binds to GSK3 but not to LRP6. **A)** Co-immunoprecipitation of HEK293 STF WCL using MYC-tagged DYRK2 to pull-down MBP-tagged GSK3. Model of hDYRK2 enhancement of GSK3 catalytic activity on LRP6. DYRK2 binds to GSK3 and increases its ability to phosphorylate the intracellular domain of LRP6. **B)** Co-immunoprecipitation of HEK293 STF whole cell lysates (WCL) using MYC-tagged DYRK2 to pull-down VSVG-tagged full length LRP6. COIP's were conducted using lysates from untreated and Wnt3a treated HEK293 STF cells. **C)** Model of DYRK2 regulation of GSK3 directed LRP6 phosphorylation.

Future Directions

My current studies provide strong evidence that hDYRK2 participates in canonical Wnt signaling. We show that hDRYK2 1) potentiates Wnt3a-mediated activation of the Wnt pathway in cultured cells (as evidenced by enhanced TOPFlash activity), 2) induces axis duplication in Xenopus embryos, and 3) promotes the phosphorylation of LRP6 on ser1490 (an indicator of receptor activation). Further studies, however, will be necessary to fully establish that DRYK2 is a bona fide Wnt pathway component. For example, it will be important to confirm that hDRYK2 activates endogenous Wnt targets. This can be simply accomplished by isolating mRNAs from cultured mammalian cells transfected with hDYRK2 and performing qPCR analysis of Wnt target genes (e.g. *Axin2*, *Fzd*, *Dickkopf*, and *TCF-1*). It will be important to demonstrate that loss of DYRK2 function impairs transduction through the Wnt pathway. We have shown that the small molecule DRYK2 inhibitor, INDY, inhibits Wnt signaling. Because INDY inhibits all members of the DYRK kinase family, inhibition of the Wnt pathway by INDY may be due to inhibition of another member of the DYRK family (Ogawa et al., 2010). Alternatively, inhibition by INDY may be due to its off target effects. To date, we have been unsuccessful in substantially knocking down hDYRK2 in human cultured cells with the 2 siRNA we have obtained. Further attempts at knocking down hDYRK2 will necessitate testing other siRNAs. If these further attempts are unsuccessful, CRISPR/Cas9-mediated gene editing to knock out hDRYK2 may be warranted.

My current hypothesis is that DYRK2 acts as a priming kinase for subsequent GSK3 phosphorylation on the ICD of LRP6. While I have shown binding of DYRK2 to GSK3 using HEK293 STF cell lysate, I have not shown binding using purified protein in a purely *in vitro* system. A CoIP using purified hDYR2 and GSK3 is needed to show direct binding. In addition, if hDYR2 targets the ICD of LRP6, phosphosites on LRP6 specific to hDYRK2 should be identified using mass-spectrometry. After these phosphosites are identified, a phosphosite mutant of LRP6-ICD specific to the target site of DYRK2 should be generated. If this site is critical for DYRK2, kinases assays using this phosphosite mutant should show a reduction in activity.

If DYRK2 binds to LRP6, multiple assays should show DYRK2 in association with LRP6 in HEK293 cells. A GFP-tagged construct of DYRK2 should be generated and co-transfected along with a YFP-tagged construct of LRP6 into HEK293 cells. If DYRK2 associates with LRP6, co-expression of the two proteins should occur. Also, analysis of sucrose density gradients of HEK293 transfected with DYRK2 should show DYRK2 associating with the same cell fraction as LRP6 if the two proteins associate in the cell.

While I have shown that hDYRK2 is sufficient for axis duplication in *Xenopus* embryos and that hDYRK2 can rescue a MOxDYRK2 posteriorization phenotype, I have not shown that this posteriorization phenotype can be rescued with Wnt signaling pathway activation. To test if DYRK2 knock-down affects Wnt signaling, MOxDYRK2 treated embryos should be rescued with other pathway components that operate at the membrane, such as LRP6-ICD which is constitutively active (Cselenyi et al., 2008), or β-catenin which should be downstream of xDYRK2 activity. In addition, to my knowledge, the expression patterns of xDYRK2 have yet to be analyzed in the developing *Xenopus*

embryo. Given DYRK2's regulation of Wnt signaling, I predict that *in situ* hybridization with probes specific to xDYRK2 mRNA will overlap the expression patterns of Wnt signaling components such as β-catenin. Also, to confirm that hDYRK2 is increasing transcription of Wnt target genes in the embryo, mRNA from animal caps of *Xenopus* embryos injected with hDYRK2 should be isolated and mRNA expression levels of the mesodermal Wnt target genes *Siamois* and *Xnr3* should be analyzed. To test if there are any defects to structures specific to the hDYRK2 induced second axis, serial sections of hDYRK2 embryos should be analyzed.

Finally, there are several questions raised by this work: does DYRK2, like GSK3 and CK1, have other substrates in the Wnt pathway? Is DYRK2 overexpressed in cancer cell lines or in stem cell niches, such as the intestinal crypt? Do other close DYRK family members, such as DYRK3 and DYRK4, also regulate the Wnt pathway? Is the difference between DYRK1 and DYRK2 regulation of the Wnt pathway dependent on cellular localization of each protein? New projects based around these questions could be initiated by conducting CoIPs between DYRK and β-catenin, the Wnt signaling component GSK3 and CK1 also target. Expression patterns of DYRK2 could be analyzed using a DYRK2 specific antibody in sections of intestinal crypts and colorectal cancer. DYRK3 and DYRK4 could be injected into *Xenopus* embryos. Finally, a mutant of DYRK1 could be generated that removes its NLS sequences, forcing it to the cytoplasm. While I have focused on the mechanism of DYRK2 regulation of Wnt signaling, the developmental effects and clinical implications of DYRK2 activity are rich areas of potential study.

References

Aranda, S., Laguna, A., & de la Luna, S. (2011). DYRK family of protein kinases: evolutionary relationships, biochemical properties, and functional roles. *FASEB J, 25*(2), 449-462. doi:10.1096/fj.10-165837

Beurel, E., Grieco, S. F., & Jope, R. S. (2015). Glycogen synthase kinase-3 (GSK3): regulation, actions, and diseases. *Pharmacol Ther, 148*, 114-131. doi:10.1016/j.pharmthera.2014.11.016

Campbell, L. E., & Proud, C. G. (2002). Differing substrate specificities of members of the DYRK family of arginine-directed protein kinases. *FEBS Lett, 510*(1-2), 31-36.

Cselenyi, C. S., Jernigan, K. K., Tahinci, E., Thorne, C. A., Lee, L. A., & Lee, E. (2008). LRP6 transduces a canonical Wnt signal independently of Axin degradation by inhibiting GSK3's phosphorylation of beta-catenin. *Proc Natl Acad Sci U S A, 105*(23), 8032-8037. doi:10.1073/pnas.0803025105

Funayama, N., Fagotto, F., McCrea, P., & Gumbiner, B. M. (1995). Embryonic axis induction by the armadillo repeat domain of beta-catenin: evidence for intracellular signaling. *J Cell Biol, 128*(5), 959-968.

Gao, F. J., Hebbar, S., Gao, X. A., Alexander, M., Pandey, J. P., Walla, M. D., . . . Smith, D. S. (2015). GSK-3beta Phosphorylation of Cytoplasmic Dynein Reduces Ndel1 Binding to Intermediate Chains and Alters Dynein Motility. *Traffic, 16*(9), 941-961. doi:10.1111/tra.12304

Hanks, S. K., & Hunter, T. (1995). Protein kinases 6. The eukaryotic protein kinase superfamily: kinase (catalytic) domain structure and classification. *FASEB J, 9*(8), 576-596.

He, X., Saint-Jeannet, J. P., Woodgett, J. R., Varmus, H. E., & Dawid, I. B. (1995). Glycogen synthase kinase-3 and dorsoventral patterning in Xenopus embryos. *Nature, 374*(6523), 617-622. doi:10.1038/374617a0

Jernigan, K. K., Cselenyi, C. S., Thorne, C. A., Hanson, A. J., Tahinci, E., Hajicek, N., . . . Lee, E. (2010). Gbetagamma activates GSK3 to promote LRP6-mediated beta-catenin transcriptional activity. *Sci Signal, 3*(121), ra37. doi:10.1126/scisignal.2000647

Maddika, S., & Chen, J. (2009). Protein kinase DYRK2 is a scaffold that facilitates assembly of an E3 ligase. *Nat Cell Biol, 11*(4), 409-419. doi:10.1038/ncb1848

McMahon, A. P., & Moon, R. T. (1989). Ectopic expression of the proto-oncogene int-1 in Xenopus embryos leads to duplication of the embryonic axis. *Cell, 58*(6), 1075-1084.

Miller, C. T., Aggarwal, S., Lin, T. K., Dagenais, S. L., Contreras, J. I., Orringer, M. B., . . . Lin, L. (2003). Amplification and overexpression of the dual-specificity tyrosine-(Y)-phosphorylation regulated kinase 2 (DYRK2) gene in esophageal and lung adenocarcinomas. *Cancer Res, 63*(14), 4136-4143.

Mimoto, R., Taira, N., Takahashi, H., Yamaguchi, T., Okabe, M., Uchida, K., . . . Yoshida, K. (2013). DYRK2 controls the epithelial-mesenchymal transition in breast cancer by degrading Snail. *Cancer Lett, 339*(2), 214-225. doi:10.1016/j.canlet.2013.06.005

Ng, S. S., Mahmoudi, T., Danenberg, E., Bejaoui, I., de Lau, W., Korswagen, H. C., . . . Clevers, H. (2009). Phosphatidylinositol 3-kinase signaling does not activate the wnt cascade. *J Biol Chem, 284*(51), 35308-35313. doi:10.1074/jbc.M109.078261

Ogawa, Y., Nonaka, Y., Goto, T., Ohnishi, E., Hiramatsu, T., Kii, I., . . . Hagiwara, M. (2010). Development of a novel selective inhibitor of the Down syndrome-related kinase Dyrk1A. *Nat Commun, 1*, 86. doi:10.1038/ncomms1090

Perez, M., Garcia-Limones, C., Zapico, I., Marina, A., Schmitz, M. L., Munoz, E., & Calzado, M. A. (2012). Mutual regulation between SIAH2 and DYRK2 controls hypoxic and genotoxic signaling pathways. *J Mol Cell Biol, 4*(5), 316-330. doi:10.1093/jmcb/mjs047

Saito-Diaz, K., Chen, T. W., Wang, X., Thorne, C. A., Wallace, H. A., Page-McCaw, A., & Lee, E. (2013). The way Wnt works: components and mechanism. *Growth Factors, 31*(1), 1-31. doi:10.3109/08977194.2012.752737

Song, W. J., Song, E. A., Jung, M. S., Choi, S. H., Baik, H. H., Jin, B. K., . . . Chung, S. H. (2015). Phosphorylation and inactivation of glycogen synthase kinase 3beta (GSK3beta) by dual-specificity tyrosine phosphorylation-regulated kinase 1A (Dyrk1A). *J Biol Chem, 290*(4), 2321-2333. doi:10.1074/jbc.M114.594952

Tahinci, E., Thorne, C. A., Franklin, J. L., Salic, A., Christian, K. M., Lee, L. A., . . . Lee, E. (2007). Lrp6 is required for convergent extension during Xenopus gastrulation. *Development, 134*(22), 4095-4106. doi:10.1242/dev.010272

Taira, N., Mimoto, R., Kurata, M., Yamaguchi, T., Kitagawa, M., Miki, Y., & Yoshida, K. (2012). DYRK2 priming phosphorylation of c-Jun and c-Myc modulates cell cycle progression in human cancer cells. *J Clin Invest, 122*(3), 859-872. doi:10.1172/JCI60818

Tamai, K., Semenov, M., Kato, Y., Spokony, R., Liu, C., Katsuyama, Y., . . . He, X. (2000). LDL-receptor-related proteins in Wnt signal transduction. *Nature, 407*(6803), 530-535. doi:10.1038/35035117

Tamai, K., Zeng, X., Liu, C., Zhang, X., Harada, Y., Chang, Z., & He, X. (2004). A mechanism for Wnt coreceptor activation. *Mol Cell, 13*(1), 149-156.

ter Haar, E., Coll, J. T., Austen, D. A., Hsiao, H. M., Swenson, L., & Jain, J. (2001). Structure of GSK3beta reveals a primed phosphorylation mechanism. *Nat Struct Biol, 8*(7), 593-596. doi:10.1038/89624

Verheyen, E. M., & Gottardi, C. J. (2010). Regulation of Wnt/beta-catenin signaling by protein kinases. *Dev Dyn, 239*(1), 34-44. doi:10.1002/dvdy.22019

Voskas, D., Ling, L. S., & Woodgett, J. R. (2010). Does GSK-3 provide a shortcut for PI3K activation of Wnt signalling? *F1000 Biol Rep, 2*, 82. doi:10.3410/B2-82

Woods, Y. L., Cohen, P., Becker, W., Jakes, R., Goedert, M., Wang, X., & Proud, C. G. (2001). The kinase DYRK phosphorylates protein-synthesis initiation factor eIF2Bepsilon at Ser539 and the microtubule-associated protein tau at Thr212: potential role for DYRK as a glycogen synthase kinase 3-priming kinase. *Biochem J, 355*(Pt 3), 609-615.

Wu, C. H., Yeh, S. H., Tsay, Y. G., Shieh, Y. H., Kao, C. L., Chen, Y. S., . . . Chen, P. J. (2009). Glycogen synthase kinase-3 regulates the phosphorylation of severe acute respiratory syndrome coronavirus nucleocapsid protein and viral replication. *J Biol Chem, 284*(8), 5229-5239. doi:10.1074/jbc.M805747200